WHITE-INTERNAL-CAVITY SPHERICAL LUMINAIRE FOR THEATRICAL LIGHTING

by

Ariel Munoz

A Thesis Submitted to the Faculty of the

JAMES C. WYANT COLLEGE OF OPTICAL SCIENCES

In Partial Fulfillment of the Requirements

For the Degree of

MASTER OF SCIENCE

In the Graduate College

THE UNIVERSITY OF ARIZONA

2023

THE UNIVERSITY OF ARIZONA
GRADUATE COLLEGE

As members of the Master's Committee, we certify that we have read the thesis prepared by **Ariel Munoz**, titled ***White-Internal-Cavity Spherical Luminaire for Theatrical Lighting*** and recommend that it be accepted as fulfilling the thesis requirement for the Master's Degree.

Professor R. John Koshel Date: 12/4/23

Professor Travis W. Sawyer Date: 12/4/23

Professor José M. Sasián Date: 12/04/23

Final approval and acceptance of this thesis is contingent upon the candidate's submission of the final copies of the thesis to the Graduate College.

I hereby certify that I have read this thesis prepared under my direction and recommend that it be accepted as fulfilling the Master's requirement.

Professor R. John Koshel Date: 12/4/23
Master's Thesis Committee Chair
Wyant College of Optical Sciences

ACKNOWLEDGEMENTS

Many special thanks to Doctor Koshel, Allyn Webber, Evan Gnam, Eric Bube, Max Schweiner, Doug Franklin, Larry Gianola, and the rest of ETC for supporting me in this endeavor. Many special thanks to Mike Kiktavi and David Kinzer for being my first manager and mentors in this career field. And lastly, many thanks to Dennis Varian and the leadership of ETC, for allowing me to continue my work on this project outside of my employment with ETC.

Chapter 1 contains information gathered from a lot of class notes in the University of Arizona College of Optical Sciences curriculum and required reading. Namely notes from the illumination and radiometry courses, diagrams, and explanations of theory from the Art of Radiometry, and notes from Princeton University on scattering. This chapter also has some recounted words from optical engineers before my time that first-hand experienced the evolution of some of this technology in the workforce.

Chapter 2, in part is information gathered from discussions with the ETC Advanced Research Group and Optical Engineering teams regarding the study of color within the theatrical industry.

Chapter 4, in full was completed through work done in the grad level illumination course at the University of Arizona College of Optical Sciences. Some initial design work was done prior to that semester, but the bulk of the finalized details that would then be submitted for prototyping were completed in this course with the help and guidance of Doctor John Koshel.

Chapter 7 and beyond would not have been possible without the help of mechanical and electrical engineers from ETC, Doug Franklin and Max Schweiner, who created a working mechanical and electrical design to make building a prototype a reality. This would not have been possible without ETC giving some of their time and resources to fund this step of the process, as well as donating ARG time to do some preliminary testing in my absence.

Credit for help in the first few rounds of editing, both technical and grammatical, can be given to Larry Gianola.

Finally, credit for presenting the idea behind this project is to be given to Evan Gnam.

DEDICATION

To my wife and our many pets, past and present.

TABLE OF CONTENTS

LIST OF FIGURES

LIST OF TABLES

LIST OF ABBREVIATIONS

ETC	ETC, Inc, formerly known as Electronic Theatre Controls
LED	Light-emitting diode
BRDF	Bidirectional Reflectance Distribution Function
JND	Just Noticeable Difference
CIE	International Commission on Illumination
ARG	Advanced Research Group
CAD	Computer-Aided Design
CCT	Correlated Color Temperature
PCB	Printed Circuit Board

CPC	Compound Parabolic Collector
CAS	CCD Array Spectrometer
CCD	Charge-coupled Device

ABSTRACT OF THE THESIS

White-Internal-Cavity Spherical Luminaire for Theatrical Lighting

by

Ariel Munoz

Master of Science in Optical Sciences

University of Arizona, 2023

Professor John Koshel, Chair

Professor Jose Sasian

Professor Travis Sawyer

Evan Gnam

Since the adoption of LEDs in theatrical lighting, color mixing has become a widely pursued interest. While many methods used today can output beams with color uniformity of around 3x to 5x MacAdam ellipse distributions, a white internal cavity of a sphere can reduce the color uniformity distribution down to a 1x MacAdam ellipse mix. This white-internal-cavity sphere can serve as a theatrical spherical luminaire that will mix and project different colored sources into a single homogenized beam to serve as a light engine for theatrical fixtures. The idea is derived from the concept of an integrating sphere used for measuring illumination sources. In an integrating sphere, an external

source is shone into the sphere which has a hollowed-out cavity painted with a special white paint. The light is then mixed within the sphere by being scattered by the paint. A detector sitting at a different port then measures the light coming out of the sphere.

The idea here is that we can take multiple color LED sources and mix them within a sphere that can then project them out to be used in a theatrical lighting system.

INTRODUCTION

Theatrical lighting has undergone many changes since the advent of color LEDs. With the increase in color specific options, the ability to replicate incandescent spectrums of light became feasible, paving the way for LED theatrical fixtures. However, mixing these wavelengths into a single homogenous beam can pose a challenge. Most of the present methods will not produce as homogenous a beam as desired, or will sacrifice too much throughput, or will add too much length to the system. Often all three at once. In this research, the plan is to address inadequate mixing and overall system length.

CHAPTER 1: What is Illumination

In the field of optics, illumination is approached in a non-imaging way, which is different from the more traditional fields of optics. While lens design and imaging optics may be used and present, illumination design will usually be constrained by target areas, brightness, and uniformity. This, as a result, often requires immense computing power that was not too pragmatic until more recent times, i.e., the mid 1990s. As a result, illumination design before powerful computers and software would be very rudimentary. However, now with computers that can trace millions of rays through complex geometries in a non-sequential manner, the feats that can be accomplished have dramatically changed. One needs to only look at the evolution of automobile headlights (i.e., projector based, steerable, with conformal optics) to see how much this field has evolved in just the past few decades.

In illumination, how light interacts on a surface is studied carefully. We consider how much light that surface is emitting, absorbing, scattering, and/or distributing in any manner. As such, there are two common forms of measurement values that can be used to help define these behaviors. These values are divided into two categories, radiometric values, and photometric values.

Radiometric values center around power and can be used to describe the entire electromagnetic spectrum.

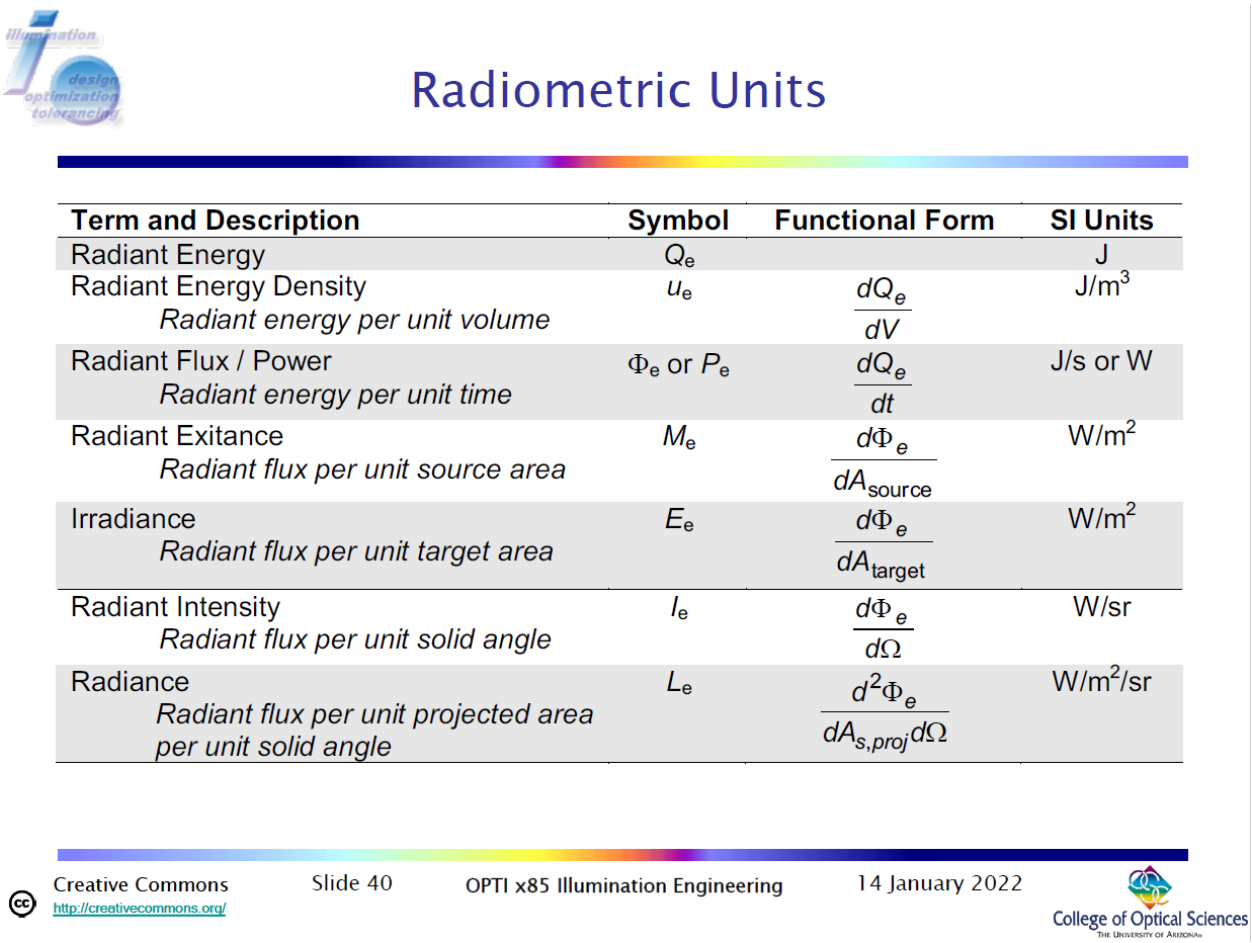

Figure 1.1: List of common radiometric units of measurements.[1]

Photometric values are focused on the wavelength band of the visual spectrum. One way to think of photometric values is that they are the visual equivalent of the radiometric units; how visibly powerful that light is to the human eye.

[1] (J. Koshel, OPTI 585 lecture notes, 2022)

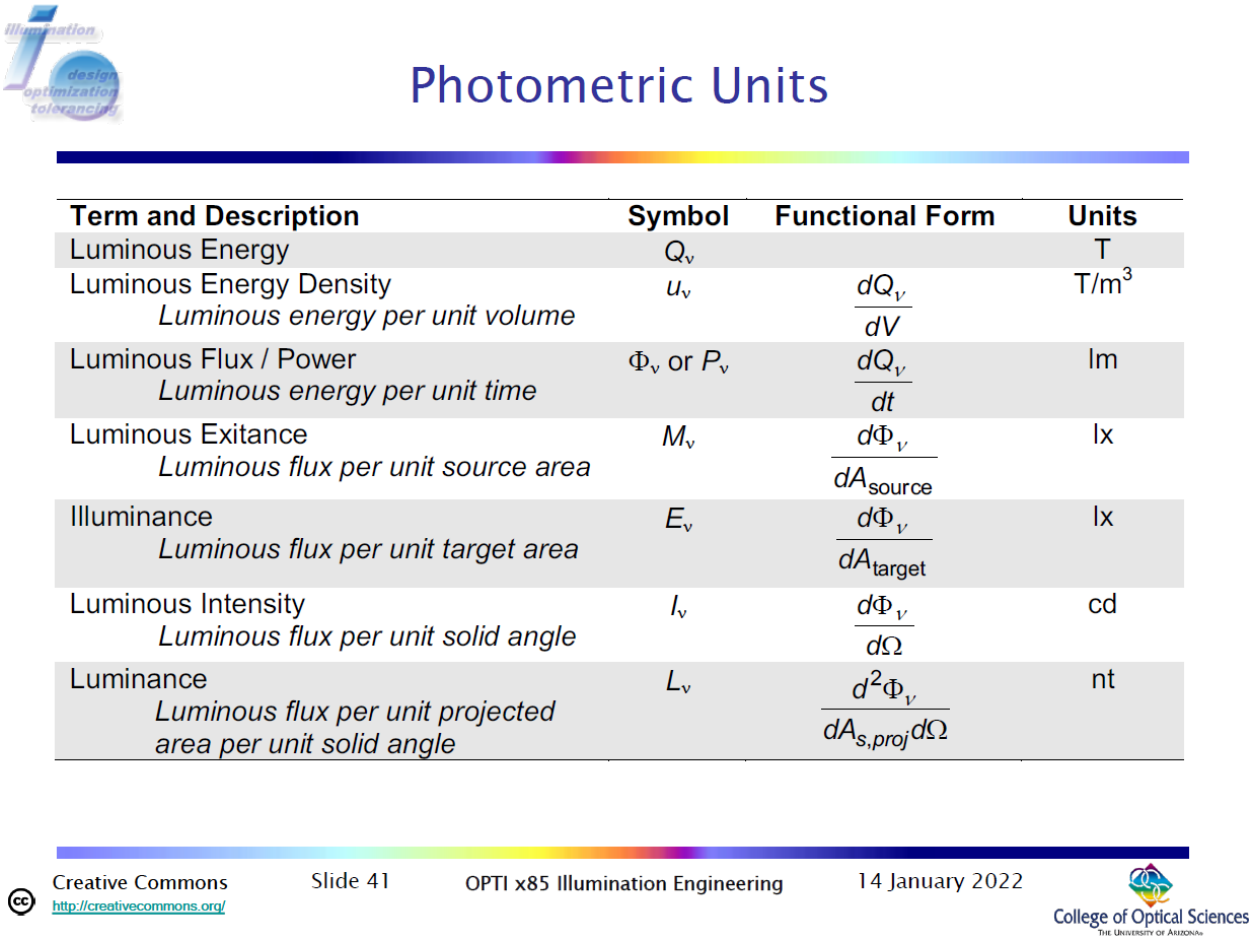

Figure 1.2: List of common photometric units of measurements.[2]

Among the most important of these units are irradiance and illuminance, radiant and luminous intensity, and radiance and luminance. In other words, the amount of power over an area, the amount of power over a solid angle, and the amount of power per area per solid angle.

[2] (J. Koshel, OPTI 585 lecture notes, 2022)

INTEGRATING SPHERES

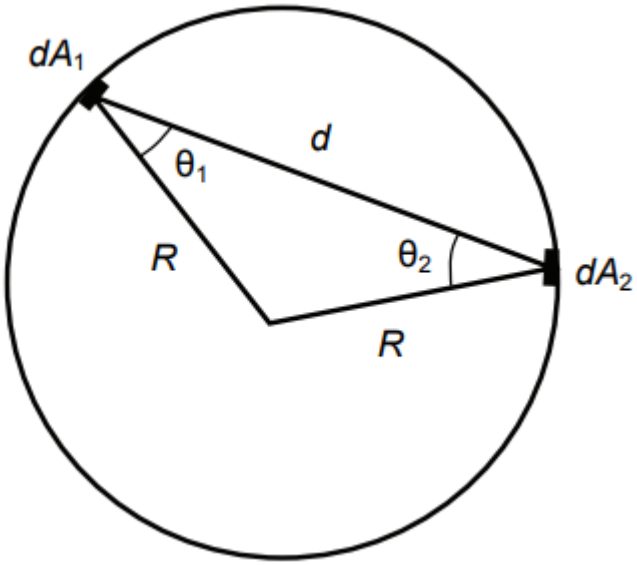

Figure 1.3: Diagram of an integrating sphere.[3]

One of the most popular ways to measure light revolves around the integrating sphere. To describe this sphere, as seen in the figure above, we can first note that $\theta_1 = \theta_2 = \theta$, and if we assume that $dA_1 = dA_2$, and that the interior of the sphere is a Lambertian surface, we can use a simplified version of the equation of radiative transfer.

$$d^2\Phi_{1\to 2} = \frac{L(\theta,\phi)dA_1\cos\theta_1 dA_2\cos\theta_2}{d^2}$$

$$\Rightarrow \qquad dE = \frac{d\Phi}{dA} = \frac{LdA}{4R^2}$$

The irradiance is constant throughout the sphere, as we can see that for any segment dA, the irradiance is only dependent on the radiance L and the radius of the sphere R, but independent of the position within the sphere, θ.

This means that if a light source were to be aimed into the integrating sphere through a port, the radiance of the sphere can be written as an expression of the reflectance of the surface of the sphere

[3] (Palmer & Grant, 2010)

coating, ρ, and irradiance. Going back to the equation for dE, it can be rewritten to give us an expression that relates the irradiance to the area.

$$L = \frac{E\rho}{\pi}$$

$$dE = \frac{E\rho dA}{4\pi R^2}$$

This expression for dE can be integrated to give an expression for the irradiance that is based on the optical power of the source light, Φ, and the reflectance.

$$E = \frac{\rho\Phi}{4\pi R^2(1-\rho)}$$

But integrating spheres are not perfect spheres, as ports are required to be able to both shine light into them, and be able to place detectors within it. The ratio of the total port area to that of the sphere, f, can be used to express the radiance as the following.

$$L = \frac{\rho\Phi}{\pi A_{sph}[1-\rho(1-f)]}$$

ETENDUE

When considering an illumination system, one of the most important system limitations can be defined through etendue. Etendue can be explained as the geometrical factor that defines the amount of light that can make it through an optical system.

To begin this discussion, the projected solid angle needs to be defined.

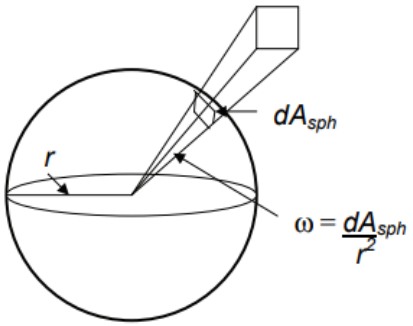

Figure 1.4: Solid-angle relationships.[4]

Referencing the figure above, we can define the solid angle, ω, with the following equations.

$$d\omega = \frac{dA_{sph}}{r^2} = \sin\theta d\theta d\phi$$

$$\omega = \int_{\phi}\int_{\theta} \sin\theta d\theta d\phi$$

However, the solid angle is a dimensionless quantity, making the projected solid-angle, which will have units of steradians, much more practical to use.

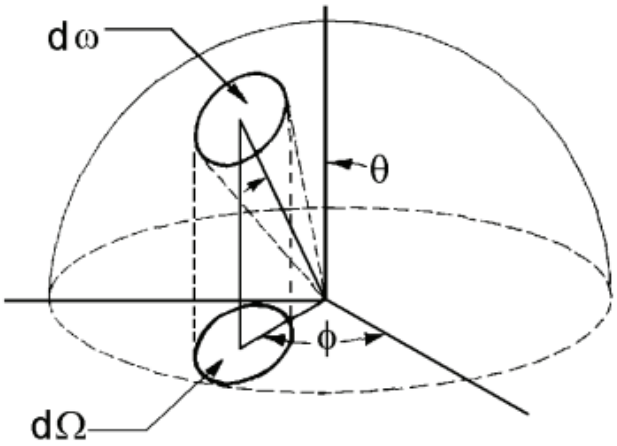

Figure 1.5: Projected solid angle relationships.[5]

[4] (Palmer & Grant, 2010)
[5] (Palmer & Grant, 2010)

Integrating over θ and φ, and applying it to a cone of light, we can get the following results.

$$\Omega = \int_{\phi}\int_{\theta} \sin\theta\cos\theta\, d\theta\, d\phi$$

$$\Omega = \int_0^{2\pi} d\phi \int_0^{\Theta_{1/2}} \sin\theta\cos\theta\, d\theta$$

$$\Omega = \pi \sin^2 \Theta_{1/2}$$

For a hemisphere of projection, this means that our projected solid angle is π sr.

Now that projected solid angle is defined, we can move on to defining etendue.

In a perfect optical system, in index n, where there is no absorption or vignetting, the amount of power through the system, assuming a Lambertian source, can be expressed as

$$\Phi = \int\int L(r,n)\, dA\, \cos\theta\, d\Omega$$

Since the source is Lambertian, $L(r,n) = L_0$

$$\Phi = L_0 \int\int dA\, \cos\theta\, d\Omega = L_0/(n_0)^2 \varepsilon$$

In this expression, ε, is what is referred to as the etendue of the system. Solving for etendue, we can then get

$$\varepsilon = (n_0)^2 \int\int dA\, \cos\theta\, d\Omega$$

In air (n=1), we can then calculate etendue at any point in an optical system with the following equation.

$$\varepsilon = A * \Omega.$$

SCATTERING

Defining scattering of a surface is usually done via BRDF (Bidirectional Reflectance Distribution Function). BRDF is a function of how light will reflect off a scattering surface defined by four variables; incoming and outgoing radiance, azimuth angle, and zenith angle.[6] In our design applications, we take BRDF files from other companies' products, or even some generated from our own samples, and apply those files to our simulation surfaces. The optical design software takes care of all the mathematical interpretation of how the light scatters upon interacting with the surface it has been applied to.

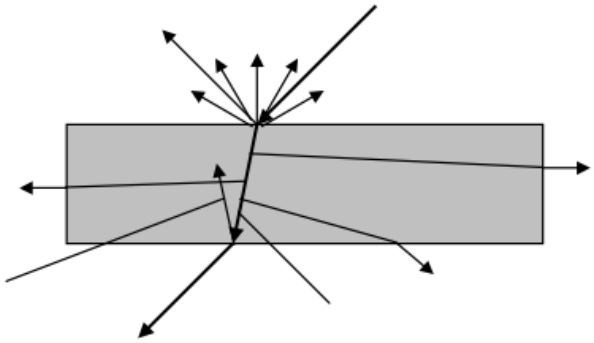

Figure 1.6: Different interactions of light between surfaces.

CHAPTER 2: Color Theory

For color mixing criteria, ETC uses MacAdam ellipses as a defined standard in evaluation. While some of our research staff have found the method to be somewhat insufficient, it is currently the best tool we have for this. A MacAdam ellipse is a region in a chromaticity chart that defines how much color difference can be perceived by the average human eye. One MacAdam ellipse is believed to be the smallest region where the average human eye can distinguish between two shades of color. 1 MacAdam Ellipse = 1 JND, Just Noticeable Difference.

[6] (Wynn, 2006)

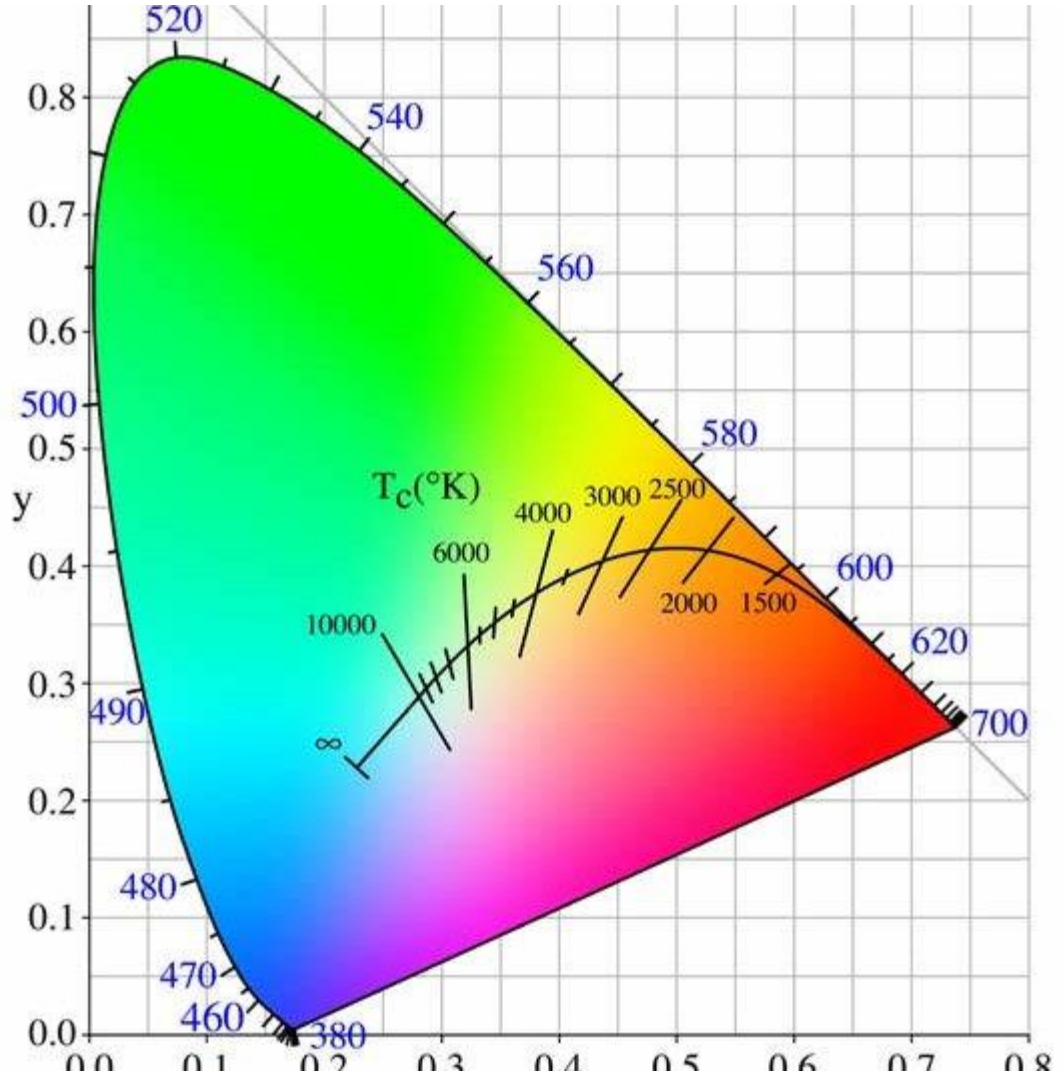

Figure 2.1: CIE 1931 xyY Chromaticity diagram.[7]

Color Gamut is the range of colors within a spectrum that a device is able to produce. In ETC applications, this is defined by the mixture and ratio of colored LEDs. To achieve specific colors, different color channels are powered at different current levels to produce the desired result. Depending on the fixture, some colors may not be achievable using these methods.

Color itself is not a measurable quantity. We have many tools to help us describe color, but we don't have a definitive measurement for color itself. Color is ultimately created by our brains, and every

[7] (Bogdan, 2011)

brain processes this information differently. The tools at our disposal give us ways to describe color, but ultimately, our perception of color is a phenomenon of our brain reading the signals the cones in our retinas receive.

CHAPTER 3: Theatrical Motivations

In theatrical lighting, color is everything! While making white light with color LEDs is generally not too difficult, theatrical applications require a much richer color gamut and mixture in order to produce natural feeling tones. Bad color gamuts, such as white light made from only red, green, and blue LEDs, on human flesh can often make the skin look unnatural or sickly. Incandescent sources would never have a problem with this as they emit across the full visual spectrum. However, color LEDs are narrow waveband emitters and much of the spectrum is lost as a result.

In order to achieve natural looking whites, more colors are added to the mix in order to replicate the full spectrum as much as possible. However, having all these narrow waveband emitters as the source, homogenizing of the light becomes a problem. As more colors are introduced, mixing the colors to improve the uniformity would require a lot more effort; longer mixing tubes, texturing the reflective material, etc. These methods often come at the cost of length and efficiency, as well as time. Designing the mixing tubes to provide a uniform beam often requires a lot of free-form molding of the curve of the tube to provide the desired beam profile. Not only that, but even after all that effort, the color uniformity is often still floating around a 3x-5x MacAdam ellipse spread, and with noticeable variance within the beam; a phenomenon colloquially described as ‘splotchiness’ in the industry.

The big concern with techniques that add length along the optical axis is that longer fixtures have been found to be unwieldy by lighting designers. Especially in smaller theaters, fixture size is an important factor to consider, especially anything that can make the fixture a long and front-heavy lever; a potential hazard to lighting designers and technicians that have to mount these fixtures at dangerous heights.

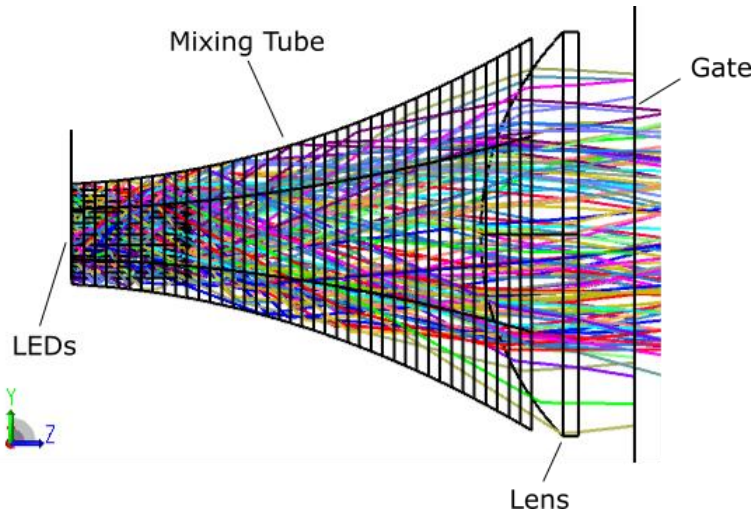

Figure 3.1: Side-view of an ETC Source Four LED Series 3 light engine optical layout.

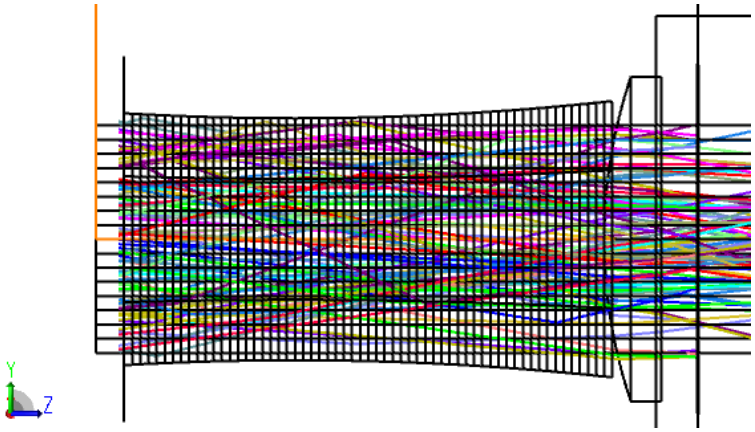

Figure 3.2: Side-view of an ETC Source Four LED Series 2 light engine optical layout.

In these two layouts above, we see the typical approach for profile lighting fixtures. An LED array followed by a reflecting mixing tube and a field lens feed into a gate aperture at the end. The gate is what is then projected and imaged onto a stage by subsequent optics. The system from the LED array to the gate is what is often referred to as a light engine, whereas any optics that follow are often bayoneted on and are swappable.

This method presents the issue that color mixture is partially dependent on the length of the reflector. The more bounces through the reflector, the more homogenized the final beam is. However, this can create dangerous cantilever geometries that can be unwieldy for lighting designers working with

limited space. While adding a rough texture to the reflector can assist in homogenizing the output with shorter overall length, it may not always be enough, and trade-offs begin to be required. Texturing also has the added disadvantage of reducing overall system efficiency. At the moment, ETC fixtures achieve approximately 50% overall system efficiency, from source to the wall/stage.

The most common color mixes achieved by ETC right now produce beams that fit within a 3x-5x MacAdam ellipse. This often requires reflector lengths in the 150-200 mm range. It is often with the aid of diffuse surfaces on these reflectors that the beams can be mixed and result in a 3x MacAdam ellipse beam homogenization.

Utilizing white surfaces can be more effective at color mixing than diffuse metallic surfaces traditionally used in reflectors. As fixtures go below 3x MacAdam ellipse beams, we begin to reach the limits of how well we can homogenize the beam with our current techniques. Currently, ETC Premier fixtures produce the following color mixes:

8 color LED array: 3x MacAdam ellipse with 26° XDLT lens tube.

6 color LED array: 2x MacAdam ellipse with 26° XDLT lens tube.

2 color LED array: 1x MacAdam ellipse with 26° EDLT lens tube.

In these cases, the 8 color LED array (Source Four Series 3 Lustr) consists of royal blue (referred to as indigo internally), blue, cyan, green, phosphor-converted (PC) amber, PC lime, red, and deep red.

The 6 color LED array (Source Four Series 3 Daylight) consists of indigo, blue, cyan, PC mint, red, and deep red.

The 2 color LED array (Source Four Series 2 Pearl) consists of 2700K white and 6500K white LEDs.

The goal here would be, at a bare minimum, to produce Lustr like mixtures that achieve Daylight mixture color performance, and Daylight like mixtures that could achieve Pearl mixture color performance.

CHAPTER 4: Spherical Solution

In order to address both color mixing requirements and shortening the light engine, a hollow sphere with matte white internal surfaces can answer both constraints. A matte white internal cavity will allow the colored sources inside the sphere to scatter off the surface and produce a nearly Lambertian

emission from the exit port. This output light can then be condensed via a CPC, field lens, condenser lens, or any other method to be fed into an optical system. As a result of the near-perfect homogenization of the light being fed from the sphere to these subsequent optics, the optics that follow the sphere can be designed solely for their intended effect rather than having to include further color-homogenizing features (i.e., reflectors can be fully specular, imaging lenses don't require achromats, etc.)

DESIGN DETAILS

The current sphere is being modeled to be a 115 mm diameter sphere with a 90 mm diameter port as defined by ETC's ARG's initial port fraction calculations[8]. The 32 LEDs are spread around in a cross-sectional layer of 2x2 arrays. This ring of 8 LED arrays around the sphere is referred to as the belt. The color mixture ratio is based on the ETC Source Four Series 3 Lustr mix ratio, which produces a 4500 K at full power across all channels.

Color LED count for 32 LED belt:

Deep red -----4

Red ---------- 6

PC Amber -- 3

Lime -------- 8

Green ------- 3

Cyan ---------4

Blue --------- 2

Indigo ------- 2

[8] (Gnam, 2020)

Chapter 5: Initial Simulation

While a lot of the preliminary research into this project (paint sampling, spectroscopy measurements, initial crude Zemax simulations) was done on ETC time, the finalization of the design for this project was worked on in the Illumination course offered at the College of Optical Sciences. The work done in this class centered heavily on nailing down the exact position of the LED belt and the inclusion of a baffle rim that will be talked about later.

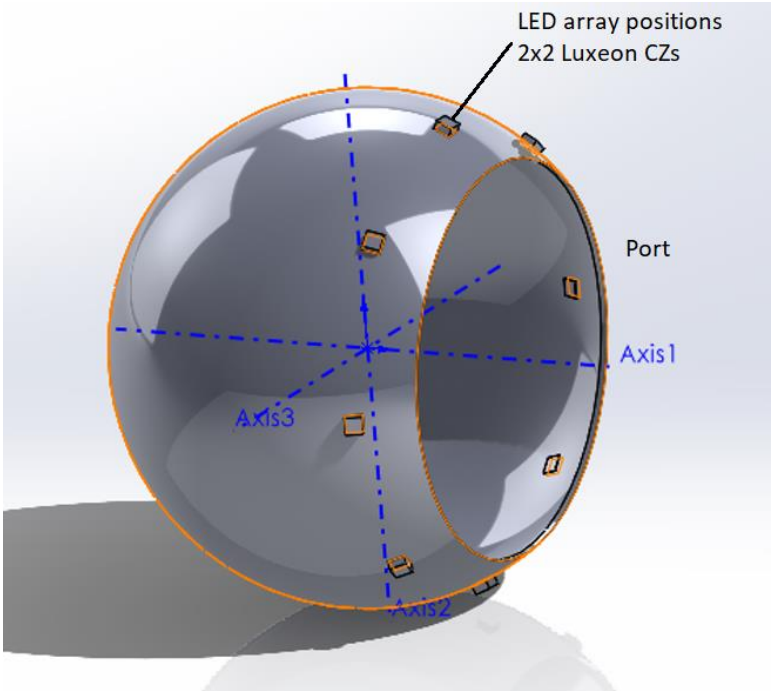

Figure 5.1: CAD file used to get the distance of the arrays from the origin of the sphere. The 8 LED arrays are colloquially referred to as the belt.

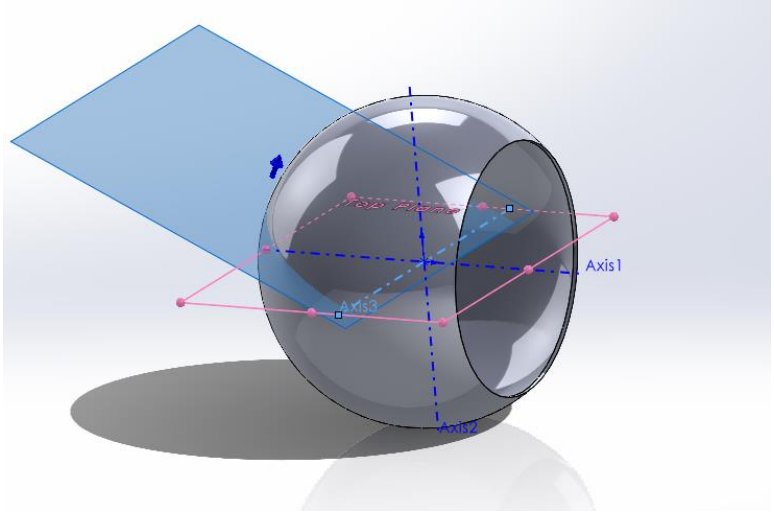

Figure 5.2: Reference sphere used to project the top array into position.

In the two figures above, the use of a SolidWorks model was used to get the exact spatial coordinates for the LED arrays to then import into Zemax. Getting both the position and tilt of these arrays with respect to the sphere was crucial to studying how well the sphere could homogenize the beam. Arrays positioned incorrectly could emit light that were aiming too high (increasing the number of bounces within the sphere and potentially missing the exit port), aiming too low (resulting in emitted light coming out directly from emitter to port without mixing), or missing the sphere altogether. This step would prove to be especially crucial in a later endeavor when a baffle rim was determined to be necessary.

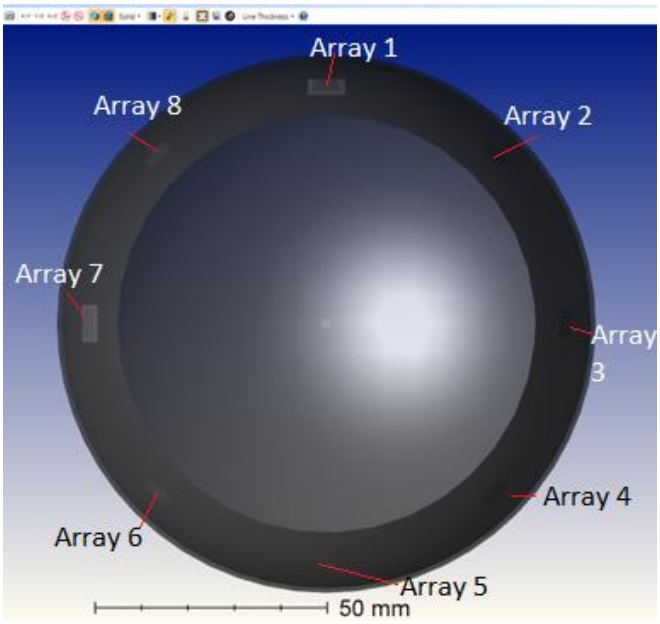

Figure 5.3: Looking into the sphere from the port side. Arrays are marked by the square surfaces.

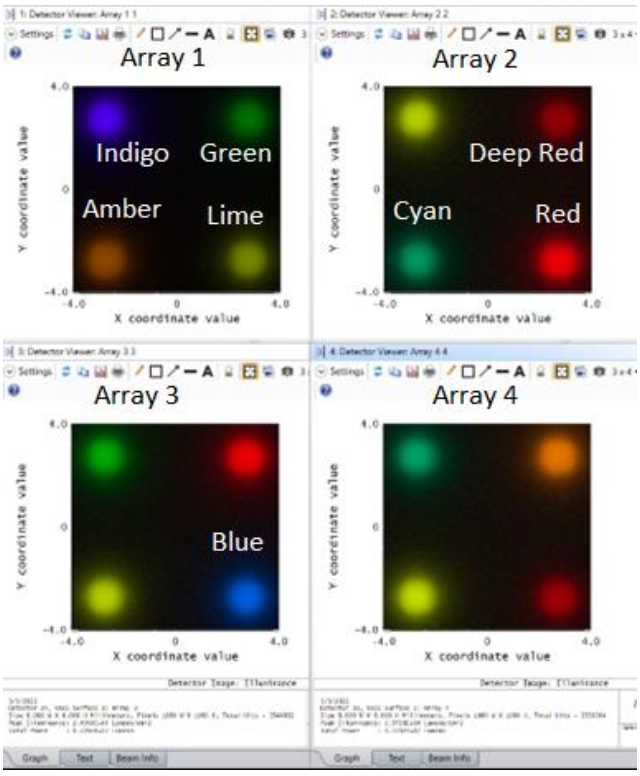

Figure 5.4: Output of arrays 1 through 4.

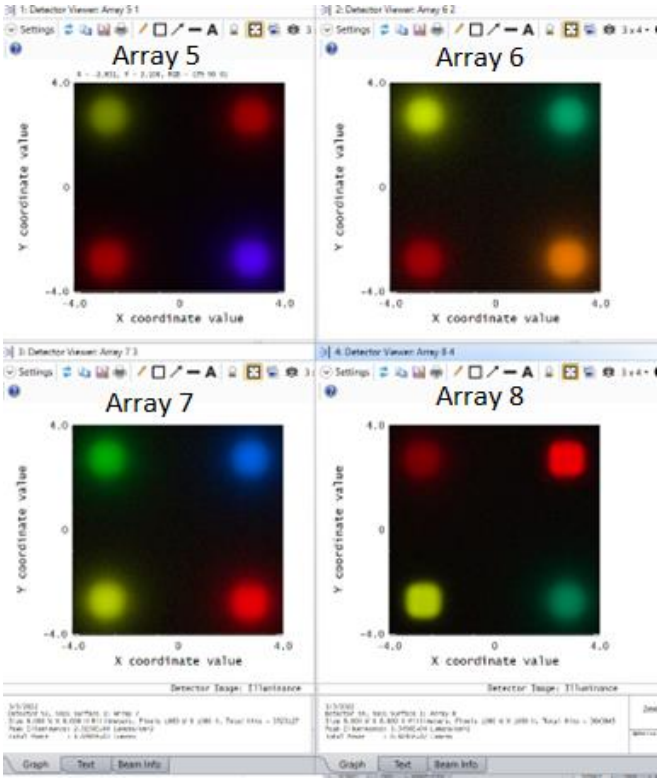

Figure 5.5: Outputs of arrays 5 through 8.

The above layout, looking into the sphere, gives the order in which the colors are distributed throughout the belt. Having the colors be as close as equally distributed as possible around the belt produces better homogenization. In past products, symmetrical color LED layouts allowed for not only better color homogenization, but also reduced any shift in CCT across the beam. Depending on the geometry of the mixing optics, this CCT shift across the beam could be gradual to the point that only a trained eye could notice it, or drastic enough that someone with no lighting design experience would still be able to notice the difference.

One advantage this design offered in the symmetrical layout around the belt was the fact that the LEDs were spread across 8 different arrays, making electrical wiring a lot more feasible, as this is often the limiting factor for color placement in larger color LED arrays, as colors need to be wired together, and space between the LEDs can only allow one or two electrical paths at most between them.

The initial simulations with this sphere, even with correctly placed, and symmetrically laid out color LEDs, resulted in a non-homogenized beam. Or rather, the central part of the beam at the port was

homogenized, but enough direct light from the LED arrays was making its way out of the sphere and creating a “splotch” effect around the edge of the beam as seen in the figures 6.6 and 5.7 below. The position of the belt was shifted to different distances from the port between the edge around the port to the equator of the sphere to find a spot where there wouldn’t be any splotch effect. However, no such optimum spot was found.

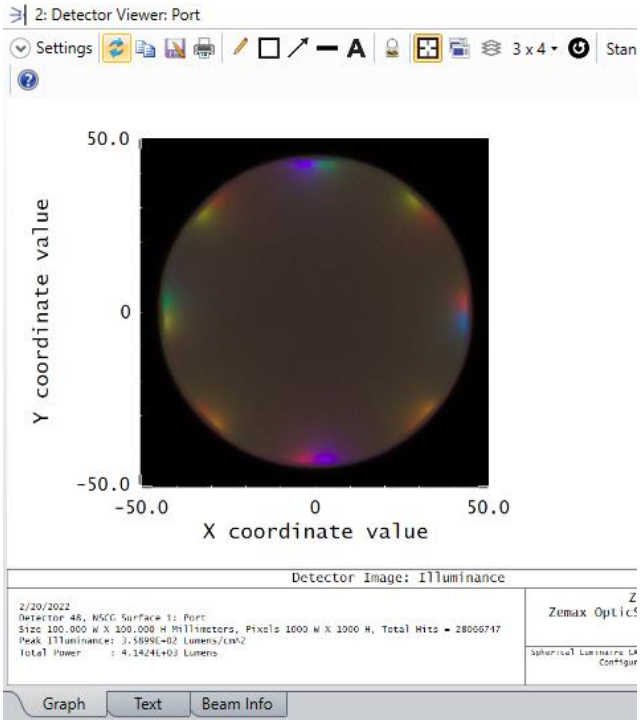

Figure 5.6: Beam at the port with the LED belt placed closest to the port.

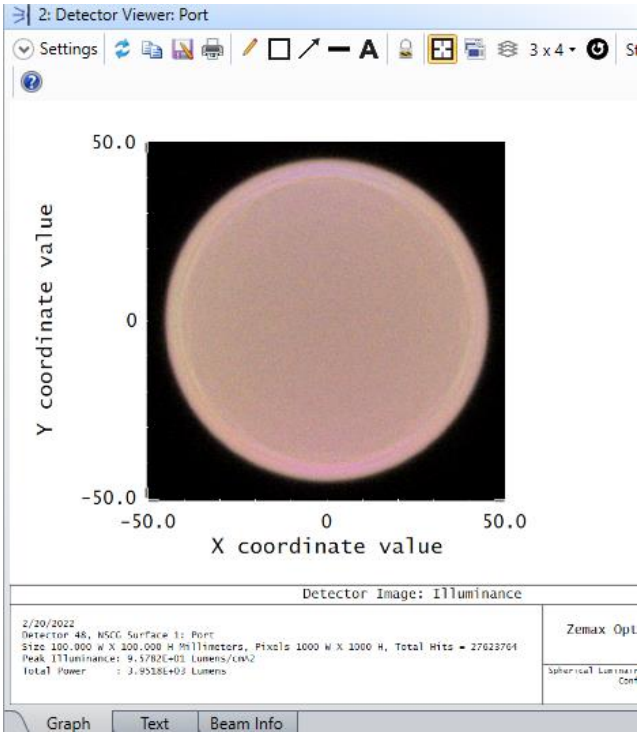

Figure 5.7: Beam at the port with the LED belt placed on the equator.

While it is true that high angle light coming out of the port would most likely be lost due to vignetting in downstream optics, we wanted to design something that could have as much of its output be as usable as possible instead of relying on trimming the edge of the beam with subsequent optics. This meant we had to figure out how to block this direct light from coming out of the port without wasting it. Initially, an idea was to add a mirrored baffle, or rim as we called it. This rim would have a well-defined angle and length to not only capture all of the light that would have otherwise directly left out of the port and reflect it back toward a coated surface, but also not create any shadows. However, it was quickly realized that fabricating such a feature would be complicated beyond our capabilities. The compromise was made to add this rim coated with the white paint. It would still reflect, but it would also be scattering the light it reflected. This would result in some drop in efficiency, but the risk was deemed acceptable for the cost savings.

Initially, out of fear of creating too much of a shadow, instead of going for a full baffle inside the spherical luminaire, small hatch-like walls were added to block the direct line of sight from LED to port.

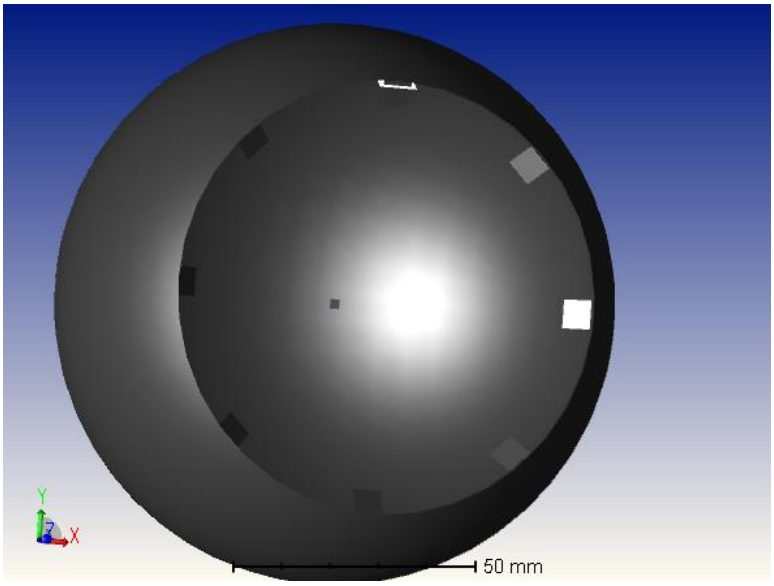

Figure 5.8: A view of the spherical luminaire port with the hatch-like walls added in front of the LED arrays.

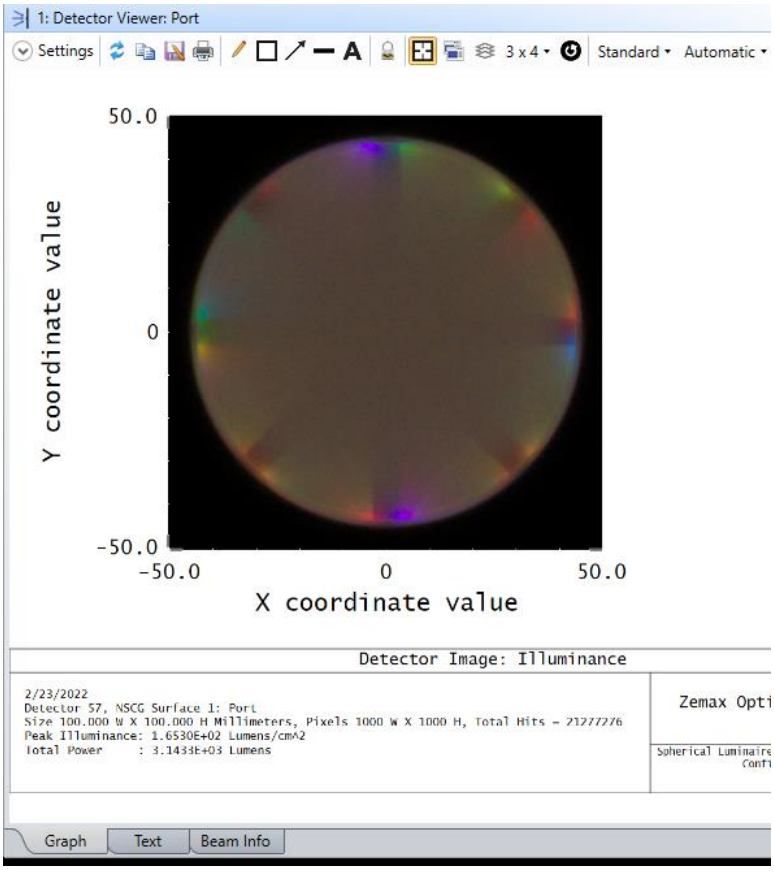

Figure 5.9: Resulting beam from adding the individual hatch-like walls blocking the LEDs.

These individual walls did not adequately block the direct light emitting from the LEDs. Additionally, unlike a continuous rim, the hatches ended up creating a more powerful shadow effect than a solid-continuous baffle would have done.

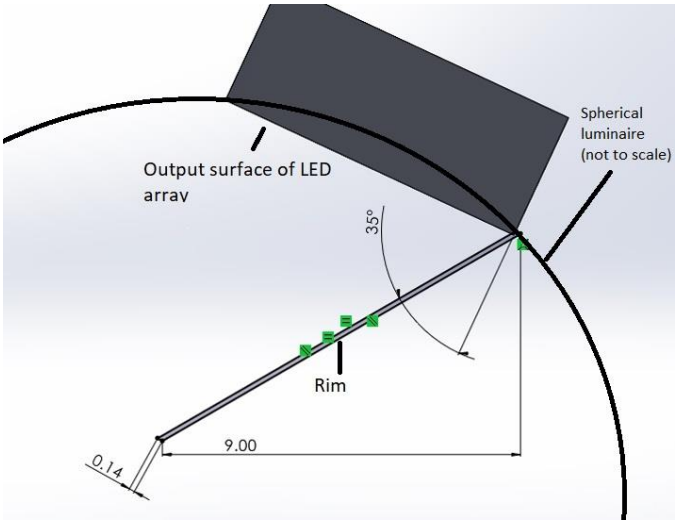

Figure 5.10: Rim design in SolidWorks.

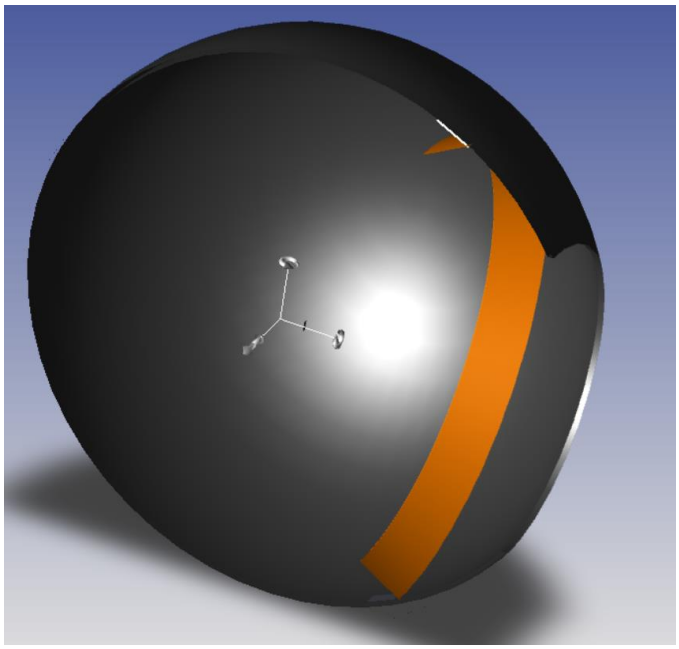

Figure 5.11: The highlighted baffle, or rim, in the Zemax 3D shaded model.

As observed in figure 5.10 above, the finalized design for the rim had it at 9 mm long and 35°from the emitter surface normal. It should be noted that the thickness of the rim in the CAD design was 0.14 mm. This was simply a placeholder to give the rim a physical thickness. The final thickness would be the minimum that fabrication methods allowed, and not exceed 2 mm, as that would begin to interfere with the light path at a noticeable level.

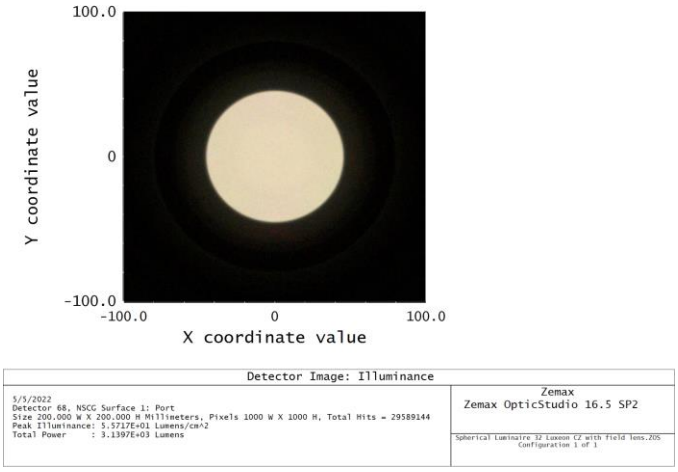

Figure 5.12: The output beam coming from the port of the spherical luminaire with the baffle in place.

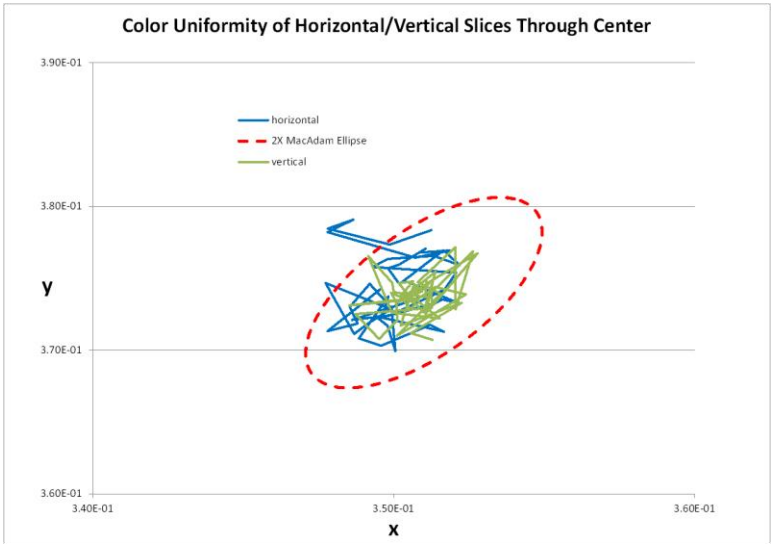

Figure 5.13: The 2x MacAdam ellipse color uniformity distribution of the spherical luminaire.

The simulation resulted with a total lumen output of 3140 lumen. Considering the total source lumens of 5222, this gives us a 76% efficiency. The beam also produced a sub-2x MacAdam ellipse

beam. However, there was concern over the large amount of stray light -colloquially referred to as a ghost ring- around the beam, as well as considerations of collecting this light outside of the port. With a 90 mm port, the cross-sectional area can be considered to be Lambertian, producing a 90° emittance half-angle from the normal. This means the etendue at this port would be enormous, resulting in major light losses in downstream optics, unless unreasonably huge optics are used.

$$\varepsilon = \pi r^2 * \pi = \pi(45\text{ mm})^2 * \pi = 19{,}985.95\text{ mm}^2\text{sr}.$$

For example, the Source Four Series 3 gate- which has a diameter of 80 mm and a 23.5° half angle cone of light projecting from the field- using $\Omega = 2\pi \times (1 - \cos(\theta/2))$, for a perfect cone[9]. The light emitting from this gate is not a perfect cone, but can be approximated to one. As a result, the etendue here can be approximated as such.

$$\varepsilon \approx \pi * (40\text{ mm})^2 * 0.52 \approx 2{,}619.5\text{ mm}^2\text{sr}.$$

The high etendue at the port creates a system limitation that cannot be adequately answered as there are many fabrication constraints in producing large diameter lenses. To date, the largest aspheres that ETC has been able to acquire that passed in-house evaluations was 200 mm in diameter. To put this in perspective, one of the standard ETC profile lens tubes has a receiving lens of 130 mm diameter and has a back focal distance of approximately 2 inches; we'll use 51 mm for this calculation.

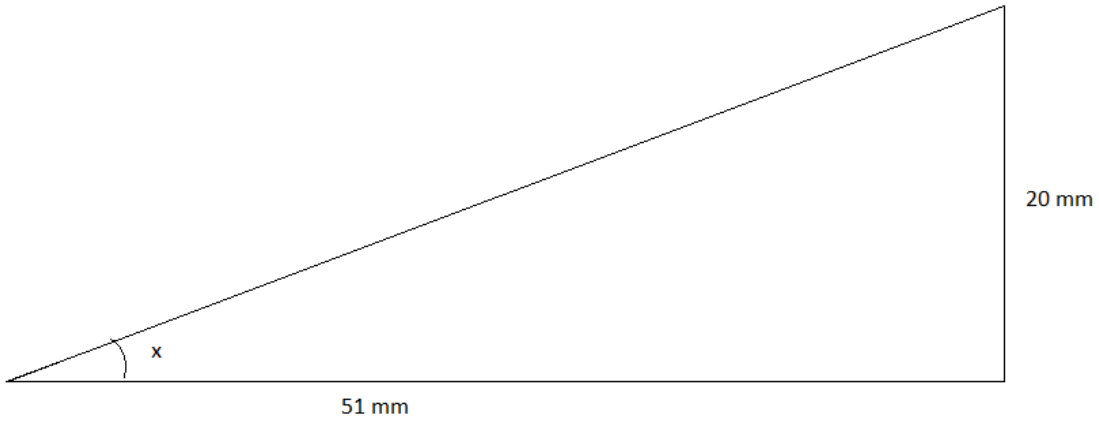

Figure 5.14: Drawing demonstrating the cone from port to edge of the 130 mm lens. 20 mm is the difference in radial height between the two elements.

[9] (*Angle Converter: Degree, Radian, Grade, Steradian, Cosinus, Sinus, Tangent*, n.d.)

$$\tan^{-1}(20/51) \approx 21.41^\circ$$

This means that any light above the 21.41° cone from the edge of the port is a loss in the system. In order to capture a 75° cone at that distance, we would need a lens of approximately 190 mm diameter; a size that approaches the maximum size of the lenses we can acquire. The input lenses for these receiving optical systems typically have 2 - 4 lenses, usually growing in size as you go farther down the system.

In order to make downstream optics more manageable, the port size can be reduced to be able to better utilize more of the light that comes out of the sphere while maintaining the collection optics at more reasonable sizes. The approach for this analysis, the LED belt location within the sphere was not changed, nor was the sphere diameter reduced in any way. In order to achieve the desired port size, cross sectional area was removed or added to the sphere until the port opening would reach the desired diameter. This is better demonstrated in the figure below.

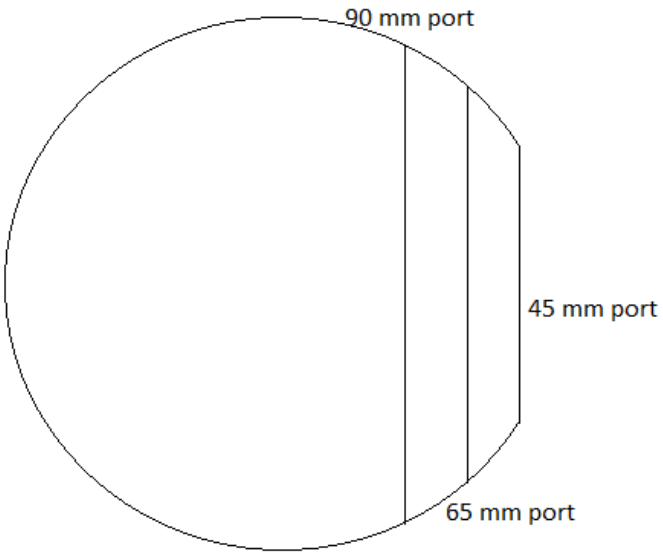

Figure 5.15: Diagram depicting the approach used to achieve varying port sizes.

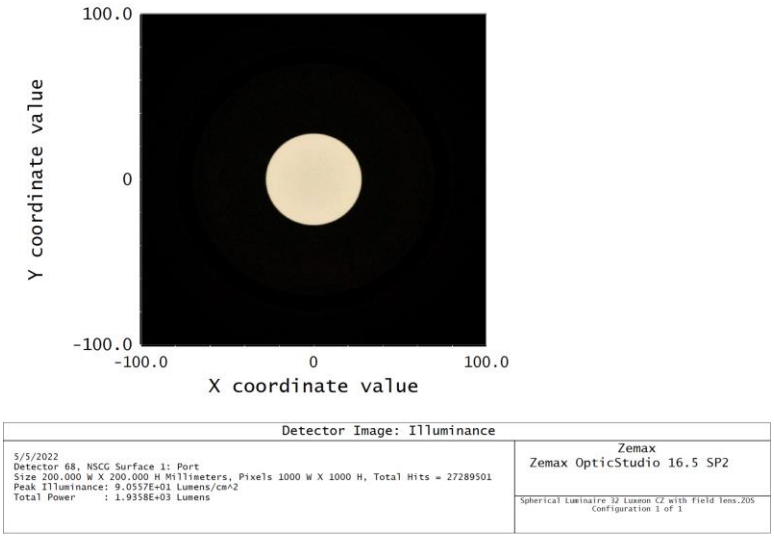

Figure 5.16: 55 mm port, 1936 lumens, 37% efficiency. Etendue = 7,463.89 mm^2sr.

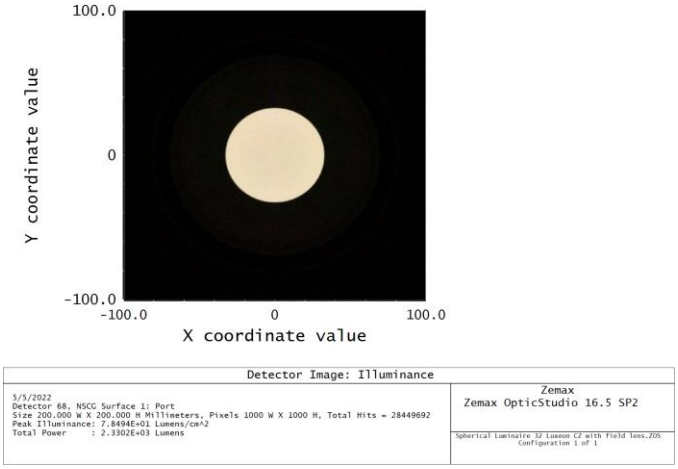

Figure 5.17: 65 mm port, 2330 lumens, 45% efficiency. Etendue = 10,424.77 mm^2sr.

The 65 mm port was chosen for a few reasons. Below 65 mm, the system efficiency quickly went below 40%, as seen in the lumen output, and the etendue was about half what we were seeing with the 90 mm port. The 65 mm port also had the advantage of producing a tighter color uniformity. While this reduction in etendue will help in collecting the light out of the port, it should be noted that it remains significantly larger than the series 3 etendue. Without the aid of reflector-based optics around the sphere's port, a lot of that light will be sacrificed; this will be discussed later.

Port Size	Etendue (mm^2*sr)	Efficiency
90 mm	19985.95	76%
70 mm	12090.27	48%
65 mm	10424.77	45%
60 mm	8882.64	41%
55 mm	7463.89	37%
45 mm	4996.49	29%

Table 5.1: Different simulated port sizes along with their etendues and optical efficiencies.

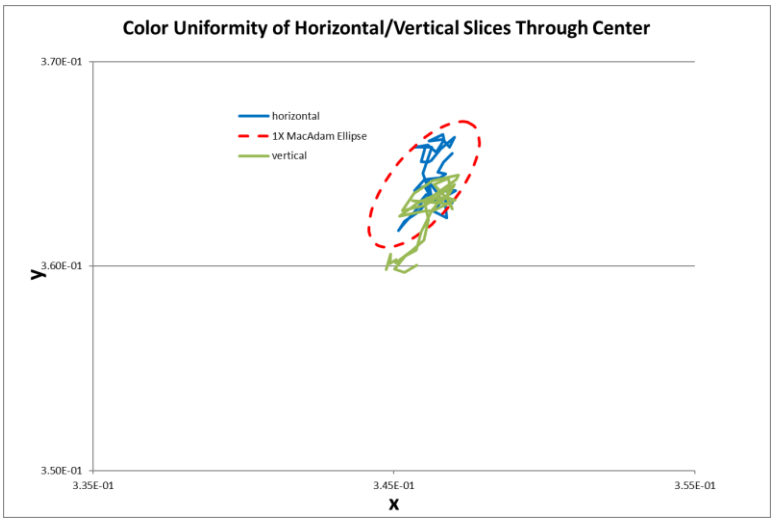

Figure 5.18: The 1x MacAdam ellipse color uniformity distribution of the spherical luminaire with a 65 mm port.

This mix fits comfortably inside a 1x MacAdam ellipse, meaning that an average/typical observer would barely be able to decern a difference in color across the beam.

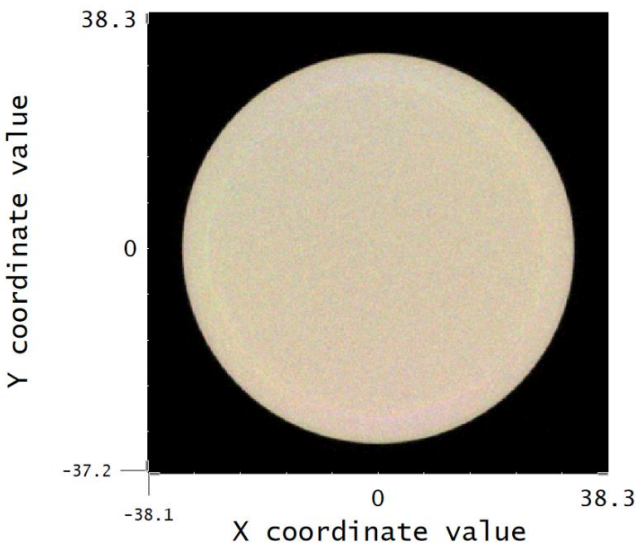

Figure 5.19: Light output at the spherical luminaire's 65 mm port. Note the discoloration of the beam as you progress toward the edge.

A quick check was done to check if the smaller port size would remove the need for a baffle, however, as seen in figure 5.19 above, this was not the case. The baffle would remain.

CHAPTER 6: Coatings

Even though the initial simulations were done using Alanod's surfaces. It was quickly determined that fabricating with such surfaces would not be cost effective. Since the surface finish of the Alanod samples is a material rather than a coating, Alanod themselves would have to build the spheres. Even if they were able to achieve the special geometry of our sphere, it would be improbable that it could be done so at a price that was feasible for ETC. This meant we needed to find an alternative solution. While we searched for alternative paint samples, Zemax simulations were performed using Alanod's F23 BRDF file as a placeholder.

The coating used will be important in the color mixing performance. While matte paints have the potential to provide the best color mixing, they may also result in the least amount of reflection, limiting the optical efficiency. For this reason, we opted to paint multiple solid plates of aluminum with different paint samples, and run spectroscopy tests on them.

The selections of paints included off-the-shelf exterior and interior paints, including some marked for stage painting. We also sampled some roof coatings, as we believed these would have higher

reflectivity in the deep violet range. Lastly, we used two in-house paint samples already used by ETC for fixture coloring. Even though we hypothesized that semi-gloss or glossy paints would not work well for this application, we included a few in order to rule them out based on lab testing.

Figure 6.1: All of the 12 initial paint samples to be measured using a spectrometer.

For these tests, we used an ideal paint sample used in integrating spheres, Spectralon, as our control.

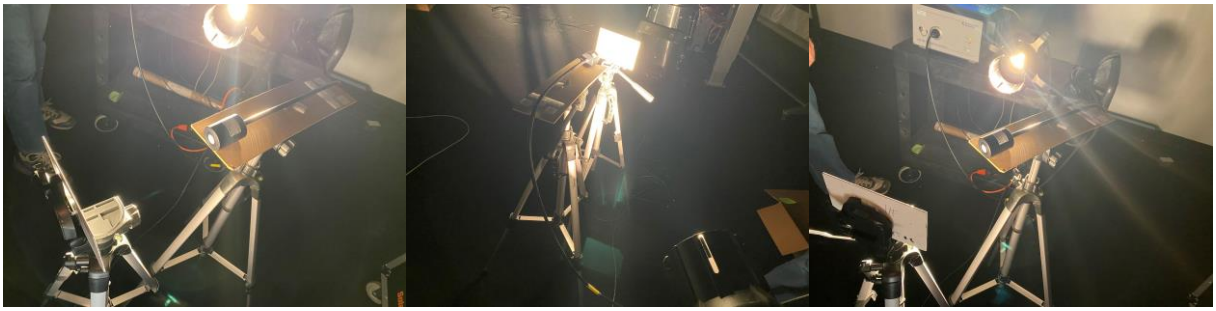

Figure 6.2: Test set up for measuring the spectral response of the 12 samples: From left to right, 1) the paint sample is rotated to be orthogonal with the detector, 2) a view from the source toward the paint sample, 3) the paint sample is rotated to be orthogonal to the incandescent source.

In this test setup, we took our painted samples and mounted them on a tripod facing an incandescent fixture using a tungsten filament; a broad-spectrum source with a CCT of 3200K. This gives us the brightest response from the white paint while also providing a full visual spectrum set of data. A

Konica Minolta CAS 140CT -151 spectrometer[10] with a cosine corrected probe was placed at an offset, aimed at the paint samples. The data was then collected again, this time with the paint samples tilted to face the spectrometer. This data was then plotted to determine which of the paint samples had the best spectral response at both angles.

Sample Number	Brand	Model number	Paint	Finish	Int/Ext	Thinning	Coats applied
1	PPG	PPG-83-610	Ceiling Paint	Flat Mate	Interior	Water	2
2	Rust-oleum	2593402 White	Traffic Striping Paint	Not specified	Exterior	Water	1
3	Behr	Barn white no. 35	Barn and Fence Paint	Not Specified	Exterior	Water	1
4	Behr	Pure White no. 1458	Marquee Ceiling Flat	Flat	Interior	Water	1
5	Behr	Ultra Pure White no. 558	Premium Plus Ceiling	Flat	Interior	Water	1
6	Behr	Ultra Pure White no. 5558	Stain Blocking Ceiling Paint	Flat	Interior	Water	1
7	Behr	White Reflective no. 65	Multi-Surface Roof Paint	Flat	Exterior	Water	1
8	Rust-oleum	Satin White 7791	Protective Enamel	Satin	Not specified	Mineral Spirits	1
9	Rust-oleum	Ultra Cover	Premium Latex Paint	Semi-Gloss	Exterior	Water	1
10	Lanco	D111	White-Seal Roof Sealer	N/A	Exterior	Acrylic based	1
11	ETC stock	PT 1004-1	Powder Coat	N/A	Not specified	N/A	ETC process
12	ETC stock	PT 1016	Powder Coat	N/A	Not specified	N/A	ETC process
13	Tucson Rubberized Coatings	Product No. 302	Enviro-Coat Roof Coating	N/A	Exterior	Acrylic based	1

Table 6.1: List of the paint samples used for testing.

[10] (*Instrument Systems CAS 140CT CCD Array Spectroradiometer*, n.d.)

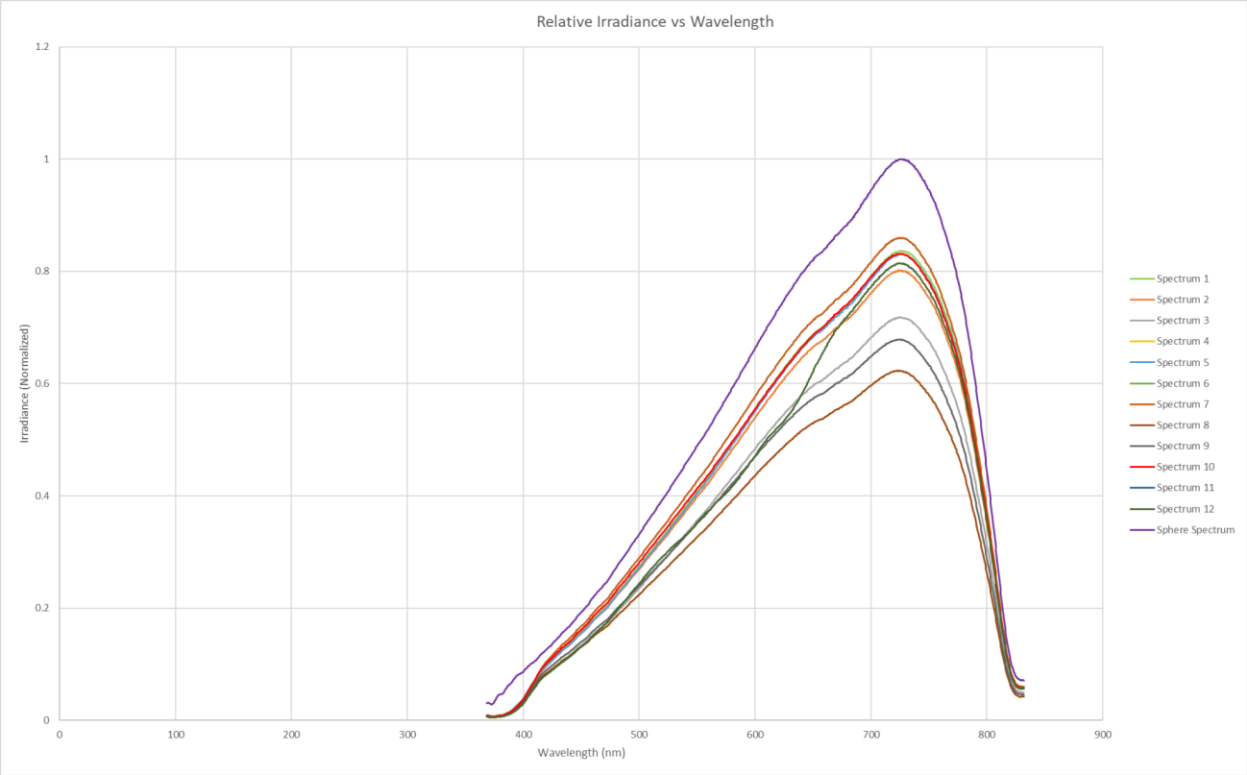

Figure 6.3: Spectrums of the first 12 samples plus the control.

The first test was done with the initial batch of the first 12 paint samples and the control sample. Sample 13 was not available yet as it was still out of stock at the time. However, from the initial test, we were able to eliminate samples 2, 3, 4, 6, 8, 9, and 11 for not having adequate performance. This left us with the final five samples we wanted to test.

By the time sample 13 arrived, we also decided to eliminate sample 12 for its relative low response in the sub-600 nm range, as this would have a negative impact on the overall color gamut. Without the blue and violet ranges being adequately represented, the color gamut would be mostly only useful for warmer color temperatures.

This left us with a final test to compare the last remaining samples; 1, 5, 7, 10, and 13.

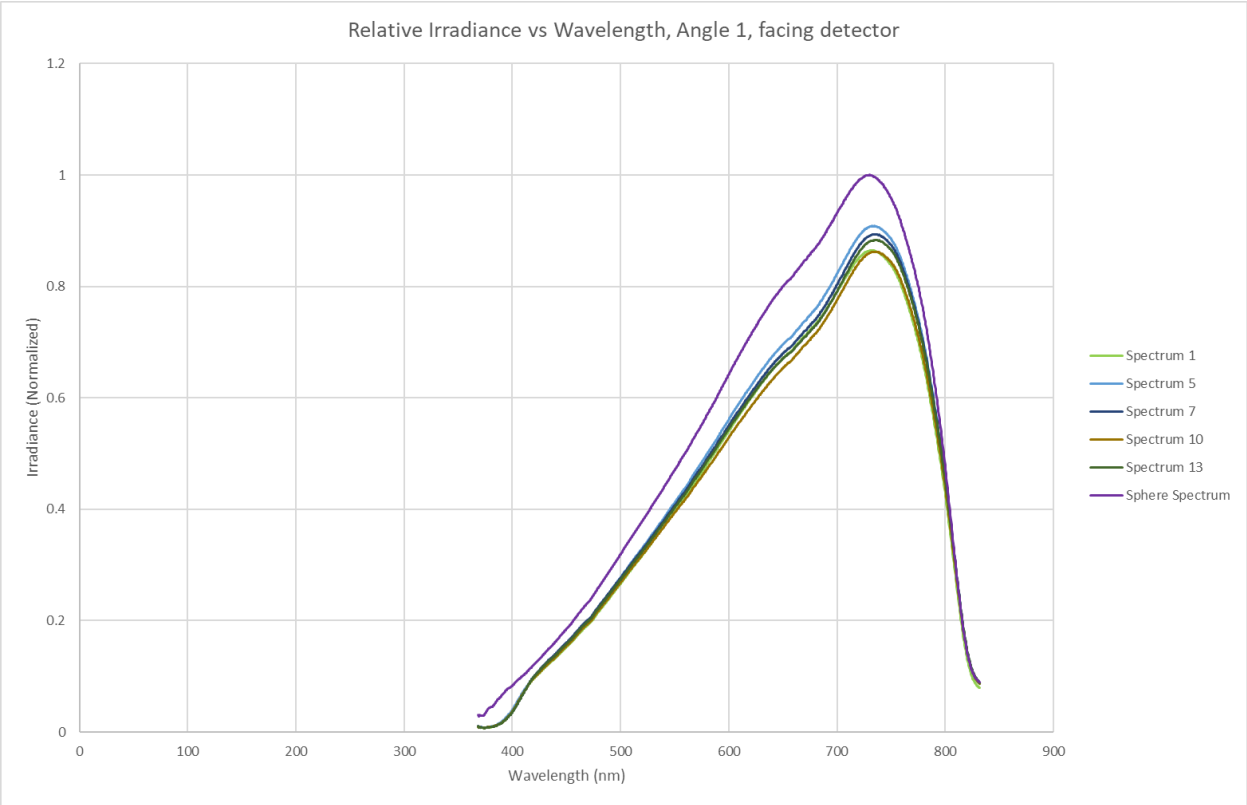

Figure 6.4: Final five spectrums, samples facing spectrometer.

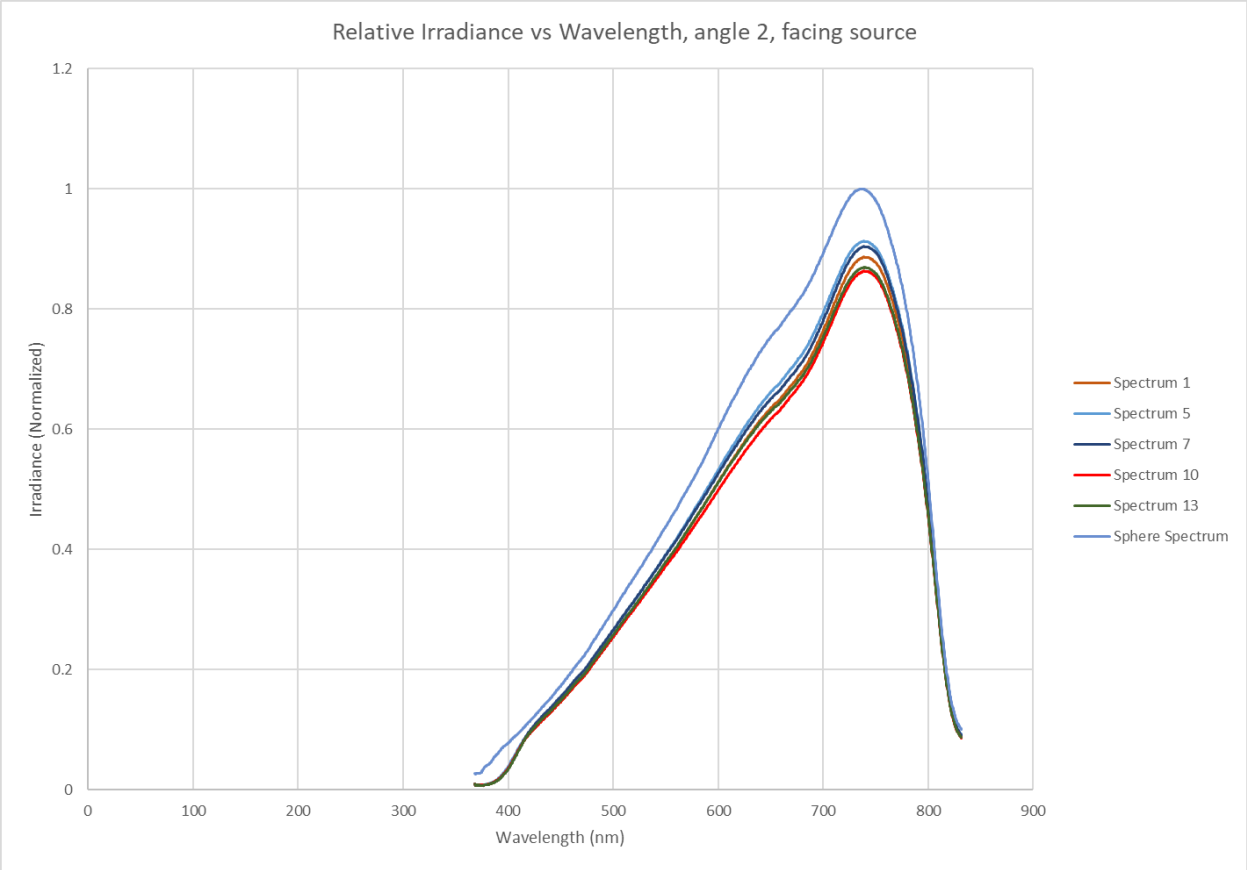

Figure 6.5: Final five spectrums, samples facing source.

From the testing, we opted to go with paint samples #5 and #7, as they had the highest response across the entire spectrum at both angles.

Between the two paints, #5 being Behr's Ultra Pure White No. 558 and #7 being Behr's White Reflective no. 65, #5 did have a slightly better response overall. However, it should be noted that #5 is an interior ceiling paint whereas #7 is an exterior multi-surface roof paint. In terms of paint durability, both in terms of temperature and optical degradation, we would suspect #7 to perform better, however, such testing is outside the scope of this project, so paint #5 was chosen for further testing in this research as it has a slightly higher spectral response.

If ETC decides to expand upon this research for production applications, environmental testing will have to be performed on these two test samples to make the final marketing decision. Unfortunately, we only had the resources to build one prototype sphere.

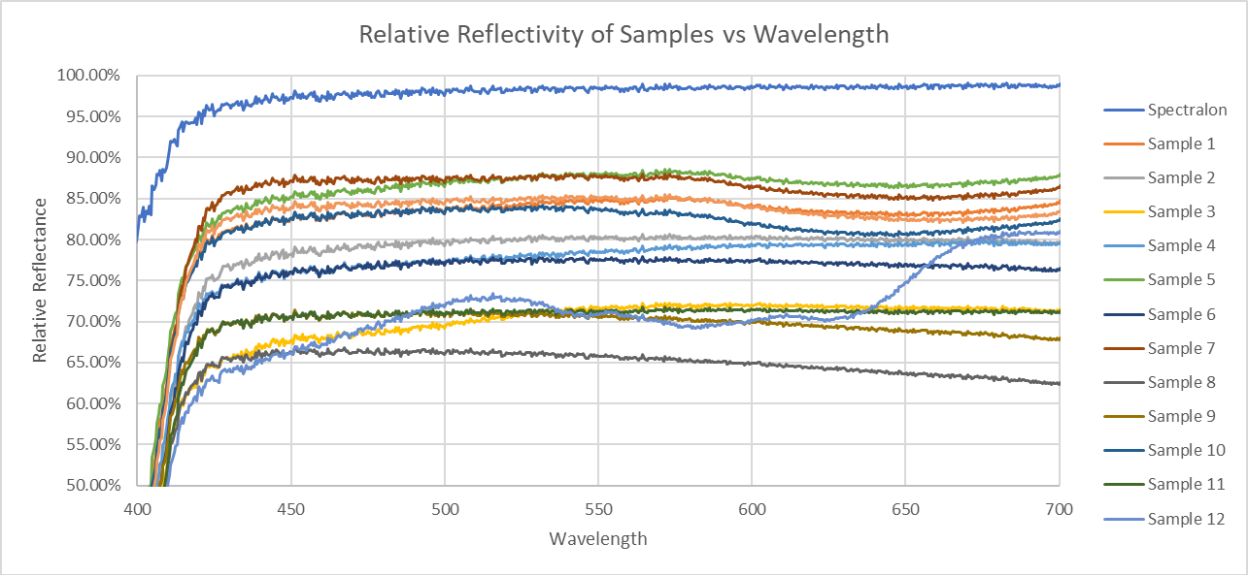

Figure 6.6: Relative Reflectance of all samples.

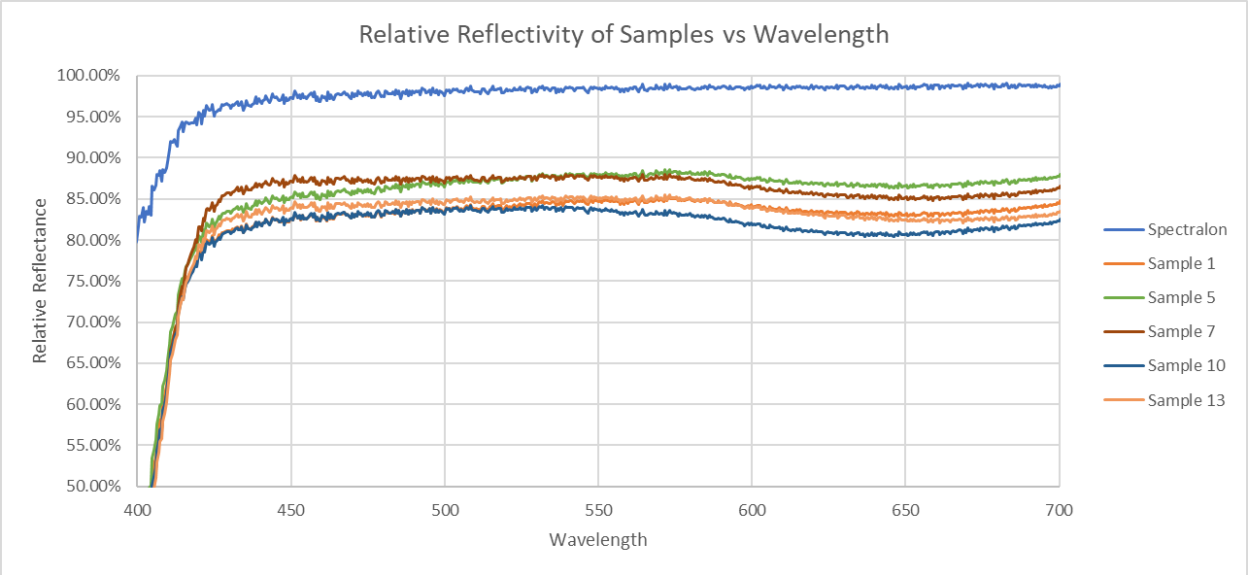

Figure 6.7: Relative reflectance of final five samples.

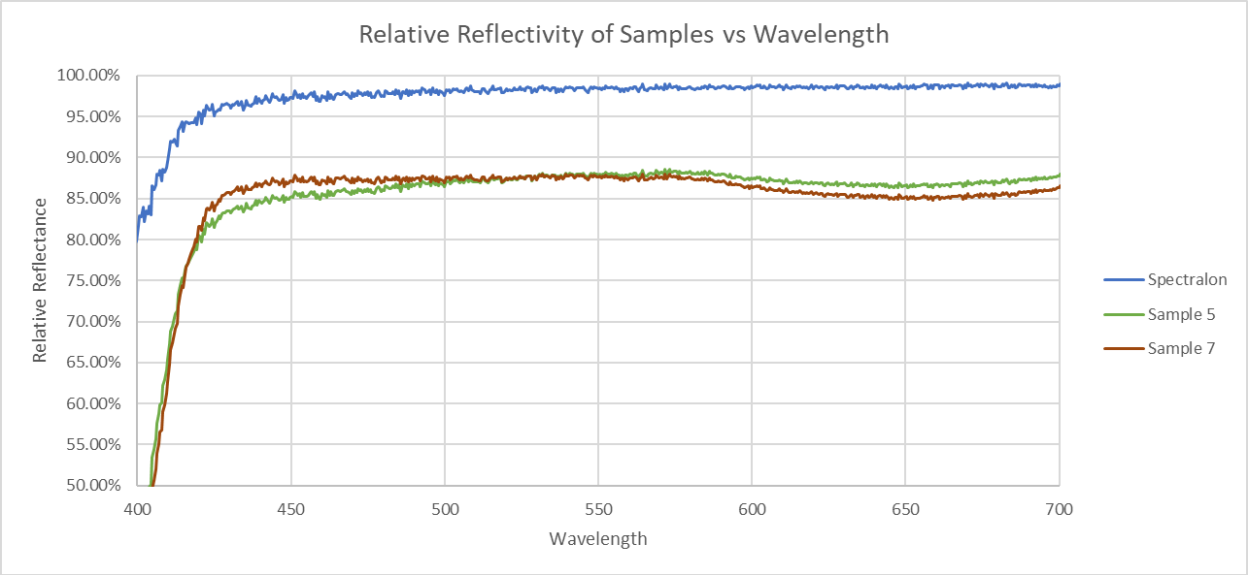

Figure 6.8: Relative reflectance of samples 5 and 7 compared to the control.

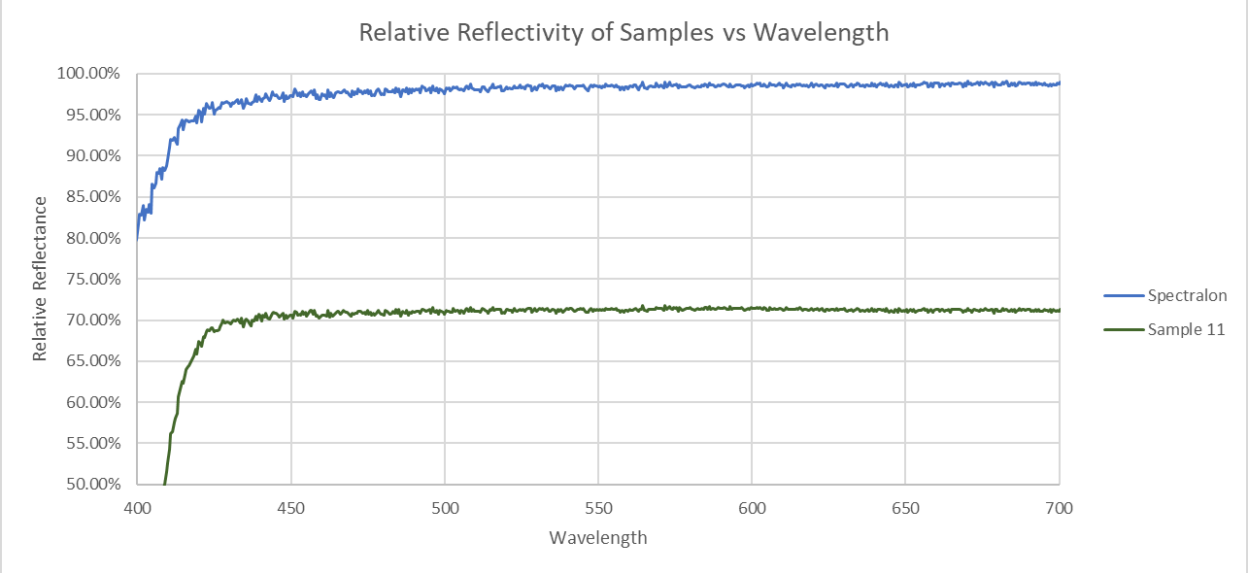

Figure 6.9: Relative reflectance of sample 11; flattest reflectance.

Additionally, we also calculated the relative reflectance of the samples. In order to do this, we took the spectrum of the incandescent source and divided all the samples' responses by the source spectrum. Getting the actual reflectance through laboratory settings requires a level of precision not

achievable with the equipment at our disposal. However, using the published data from LabSphere's website, we knew that Spectralon is expected to have a 99% reflectance within the waveband of interest.[11]

Using a multiplier, the Spectralon data was adjusted to reflect the published specifications. All other samples were then adjusted by the same multiplier. Leaving us with a relative visual comparison of reflectance. Two big conclusions were drawn from this data. The overall highest reflectance achieved by the paint samples were about 12% less than Spectralon's reflectance, and, even though paint samples 5 and 7 were the highest in reflectance, their reflectance curve was not as flat as one would desire. This could have some negative implications to the adjustability of color tuning as individual channels are turned on or off in a fixture. However, this can also be controlled with software to negate uneven sensitivities across the spectrum.

Interestingly enough, sample 11, which is one of ETCs powder coat samples, had one of the flattest reflectance curves of all the samples. However, this sample also had one of the lowest overall reflectance values, with about 27-29% loss compared to the Spectralon.

While none of these samples come close to having as high of a reflectance as Spectralon, the cost savings are immense. Off-the-shelf paints are made with cheaper and easier to work with ingredients to make their shades of white; whites whose only purpose is for decorative reasons. Spectralon however, is made with carefully selected ingredients to produce a high optical quality matte coating that is highly reflective across the entire visual spectrum. These are considerations that are absent in the making of regular off-the-shelf paint, where mass production and low cost take priority. Off-the-shelf paints will have a higher probability of having the ends of the visual spectrum absorbed and may not always be as matte as a special-made material like Spectralon.

CHAPTER 7: Prototype Sphere

In order to be able to paint the internal surfaces, it was decided that the sphere would be built in two hemispheres, and then they could be assembled once the paint had been applied. After some discussion with machine shops, the prototype sphere was built out of aluminum by Proto Labs using DMLS (Direct Metal Laser Sintering)[12], a metal 3D printing process.

[11] (*Spectralon® Diffuse Reflectance Targets Durable Reflectance Panels for Laboratory and Field Applications under Harsh Conditions*, n.d.)
[12] (*Metal 3D Printing Service for Custom Parts | Online Quoting*, n.d.)

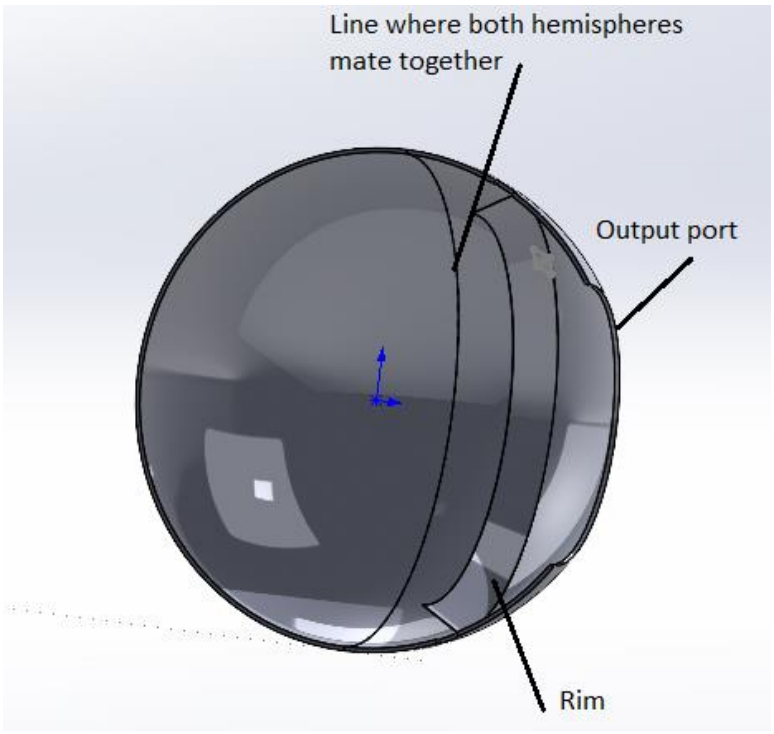

Figure 7.1: Segmented view of the spherical luminaire halves.

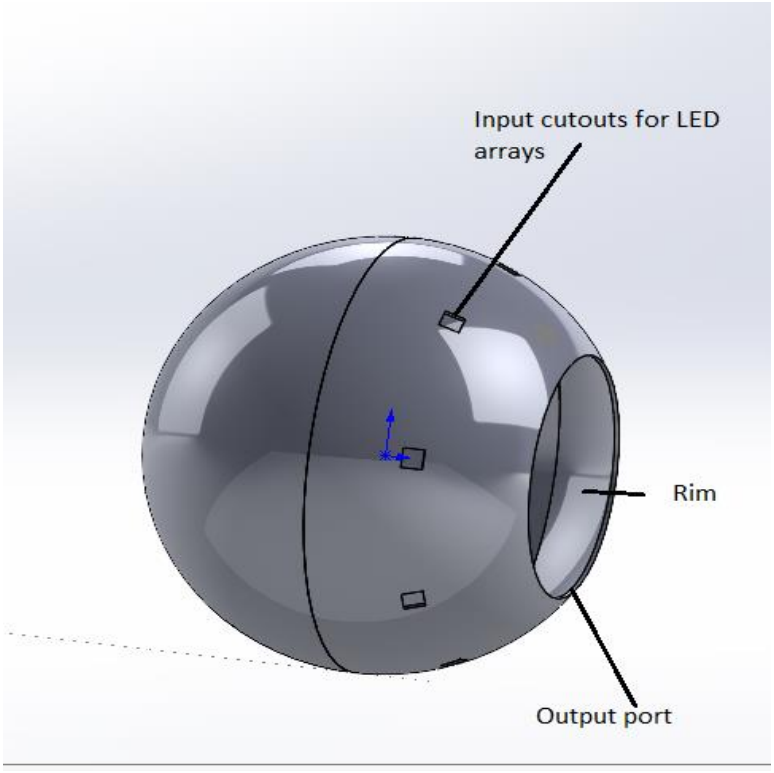

Figure 7.2: Spherical luminaire.

Once the spheres were completed, they were sent to my home in AZ in order to be painted. The painted samples were then shipped back to ETC in WI for final assembly.

Figure 7.3: A view of the internal structure of the spherical luminaire, front(right) and rear (left).

Figure 7.4: Interior section of the rear side of the spherical luminaire; note the texturing as a result of the fabrication method. This may be later addressed with different fabrication methods.

Figure 7.5: Interior of the front side of the spherical luminaire. The LED array slots can be clearly seen as well as to how the baffle stacks right against them.

Figure 7.6: Exterior of the front side of the spherical luminaire. Showing flange for cooling fin attachment.

Figure 7.7: Exterior of the rear side of the spherical luminaire. Showing flange for cooling fin attachment.

Figure 7.8: Spherical luminaire sections painted.

During the time the spheres were being fabricated and painted, the ETC electronics and mechanical teams were hard at work creating the cooling fins that would also act as the LED PCB mounts. The fins used an L-shape structure, with one leg being used to interface the LED PCBs into the spherical luminaire ports, and the other leg to house multiple fins to act as heat sinks. This LED PCB and cooling assembly was ready to be installed by the time the painted segments of the spherical luminaire had arrived back in Wisconsin.

Figure 7.9: Multiple LED array PCBs were constructed for each of the eight array configurations.

Figure 7.10: LED PCB mounted directly on to the fin. This is ready to be installed onto the spherical luminaire.

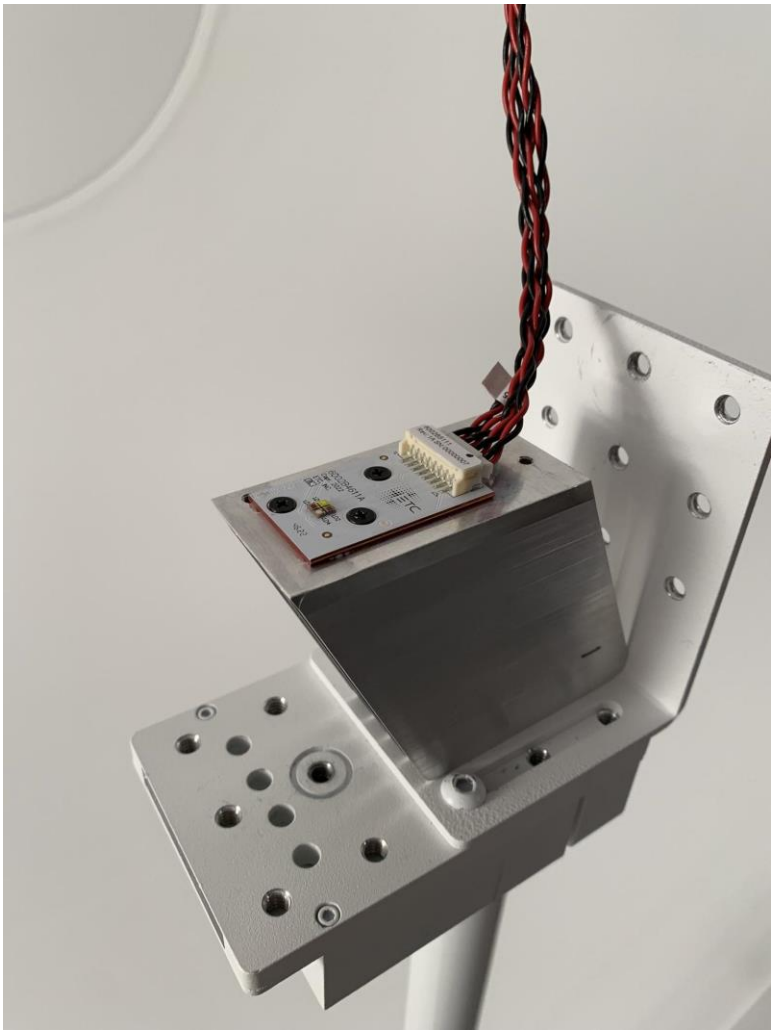

Figure 7.11: Side view of the L-shaped LED PCB and heat sink assembly.

The LED arrays were all individually mounted to L-shaped heat sinks. These heat sinks would then interface with the sphere upon final assembly. While the heat sinks in this prototype are quite large, their size can be reduced with the introduction of fans. At the moment, for prototyping purposes, the heat sinks would rely on passive convection cooling.

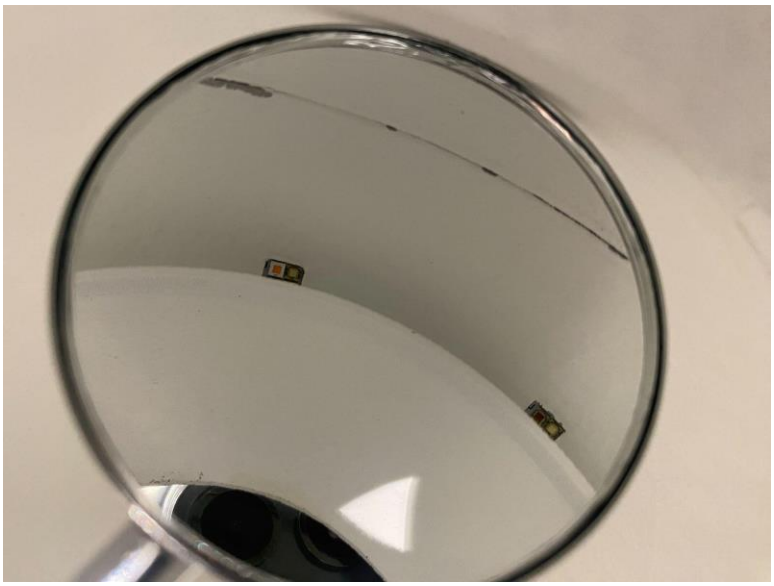

Figure 7.12: LED arrays protruding through the ports. These ports were made to be almost exactly the same size as the array to maximize the scattering surface area in the internal cavity.

Figure 7.13: A view of the LED arrays powered on while in the sphere.

Care was taken to minimize how much the LED arrays protruded into the internal cavity of the spherical luminaire, as this would create shadows. The LEDs in this assembly sit just shy from flush as seen in the picture. Further mechanical adjustments could be integrated into the assembly in the future to get them perfectly flush.

Even though the ports for the LED arrays were sized to be just enough space for the LEDs to clear, white PCB boards were used for the little bit of space left between the spherical luminaire and the edge of the LEDs. Even though the white material in the PCB boards is not the same scattering material used in the internal side of the sphere, it would still allow the little bit of light interacting with it to be reflected back into the sphere better than using a traditional darker green color PCB. This could be a

fraction of a percent in efficiency saving, but considering there are no negatives to choosing this PCB color, there is no reason not to go that route.

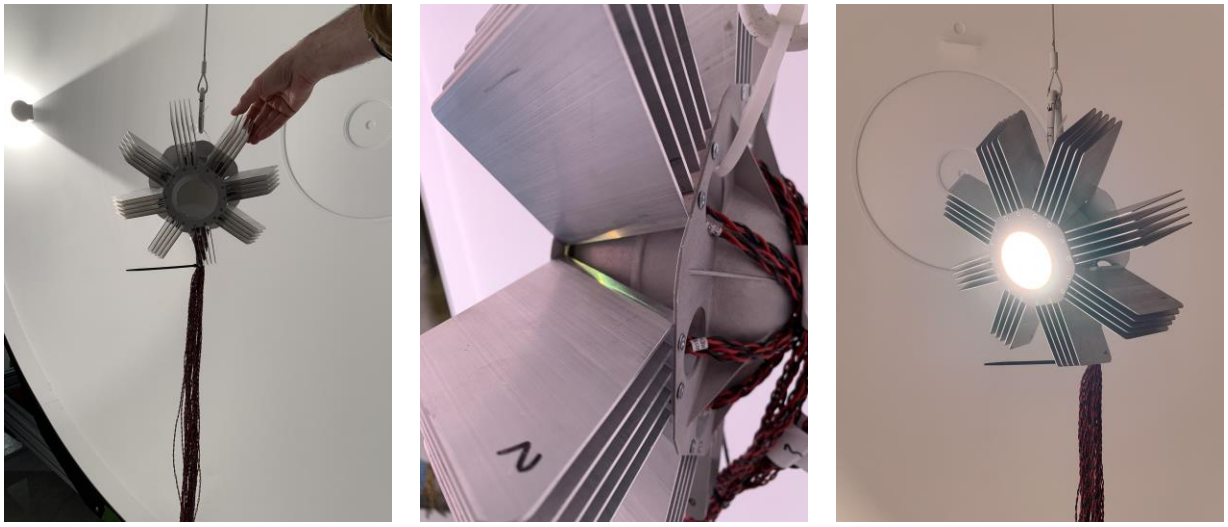

Figure 7.14: The spherical luminaire fully assembled and operating. The large Labsphere integrating sphere used for testing can be seen in the background.

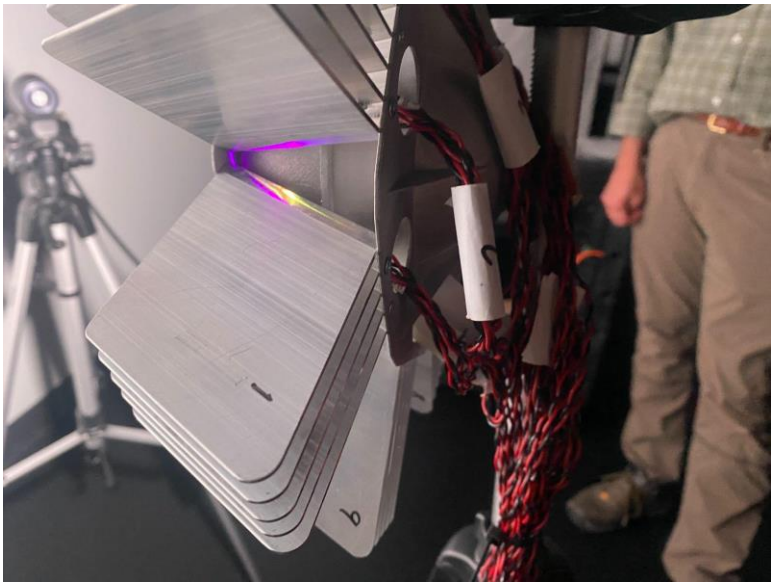

Figure 7.15: Light “bleeding” out through the ports. This is a source of loss in efficiency.

Comparing the color of light between the middle picture of figure 7.14 and the light in figure 7.15, we can observe how each individual array has its own “color”. Care was taken to distribute the visual spectrum throughout the LED belt. However, there are two things that happened that resulted in a potential degradation of color uniformity. Upon mounting the LED arrays into the sphere, one of the lime channels shorted out, making one side of the cavity noticeably more red than the rest of the cavity. The other was that a green channel was accidentally fabricated with a cyan LED. This was a mistake made in the PCB line. The decision to not rectify it was made in order to maintain momentum in the fabrication schedule. This could be fixed in later prototypes. In terms of results at this stage, the expected effect is minimal, as the cyan and green LEDs are close to each other on the visual spectrum. In terms of luminous power, we did expect this would be an observable dip as green LEDs are brighter than the cyan LEDs.

Figure 7.16: 2 meter integrating sphere from Labsphere.

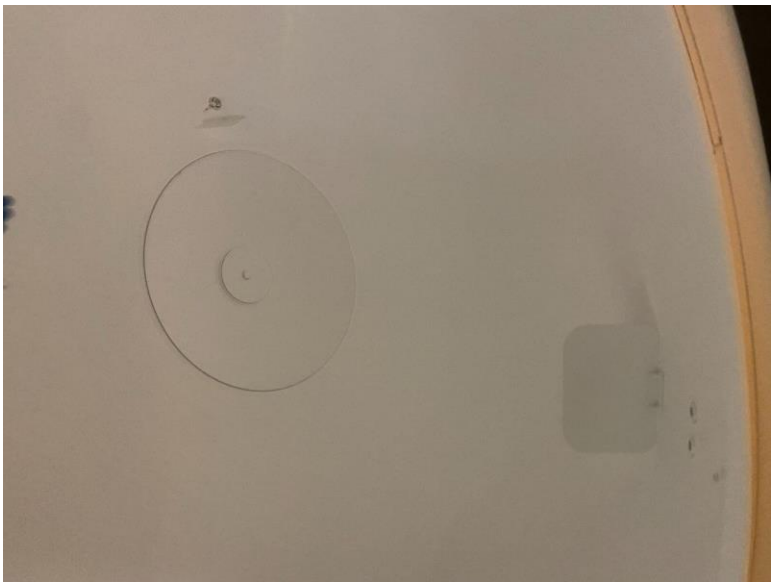

Figure 7.17: Internal structure of the 2 meter integrating sphere.

The spherical luminaire was then tested in ETC ARG's 2 m integrating sphere from Labsphere. With these measurements, we were able to get a clear picture of how good our white paint works with the luminaire.

	Bare Arrays Prior to Mounting Brightness (Lumens)									Arrays mounted in Luminaire	
Color	Array 1	Array 2	Array 3	Array 4	Array 5	Array 6	Array 7	Array 8	**Total Lumens per color**	Brightness per channel (lumens)	Efficiency
Deep Red		34		35		35		36	**140**	43	30.71%
Red	248		127	120		127	122		**744**	228	30.65%
PCAmber		207			206			194	**607**	187	30.81%
Lime	367	361	372	366	351	362	375	370	**2924**	759	25.96%
Green		138	227		229		145		**739**	382	51.69%
Cyan				140		142		177	**459**		
Blue			85				88		**173**	54	31.21%
Indigo	6				29				**35**	19	54.29%
										Sum by channel	
Total lumens per array	**621**	**740**	**811**	**661**	**815**	**666**	**730**	**777**	**5821**	**1672**	28.72%
										Sphere measurement with all channels on	
										1646	28.28%

Table 7.1: Showing the results of the individual color channels operating outside of the sphere, as well as the results once loaded into the spherical luminaire.

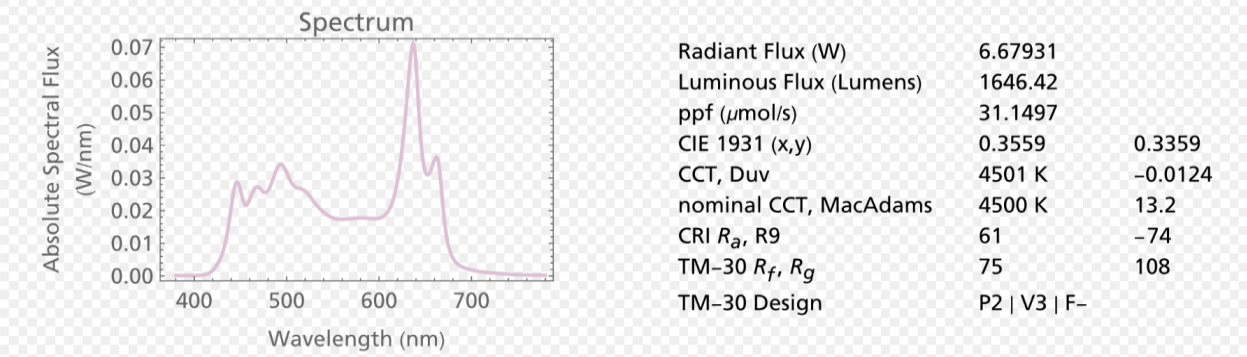

Figure 7.18: Results from ETC's ARG testing.

Our testing resulted in an overall efficiency of 28.7%. The loss in efficiency over the expected 45% can be attributed to four factors. The light loss in the crevice between the mating of the two hemispheres, and the lower efficiency of the #5 paint sample versus the F23 sample from Alanod. It can also be observed that within the gap, parts of the painted surface have chipped. The paint application itself may also not be as uniform as it would be in simulation.

Of these four factors, paint sample #5 is the easiest one to answer in simulation. After a lengthy wait, we were finally able to get the BRDF files for these samples from Optech. Running a simulation with these, we got a 31% efficiency, which means that the uneven surface, paint chips, and light loss through the side of the ports are causing around a 2.3% loss. In order to effectively gain luminous efficiency, better paint samples will be needed. 12 samples were chosen as a reasonable starting point, but much larger samples can be scouted out and tested. This would require a significant time commitment as painting each aluminum sheet took multiple hours, including cleaning out the paint gun, applying multiple coats, and dry time in between coats.

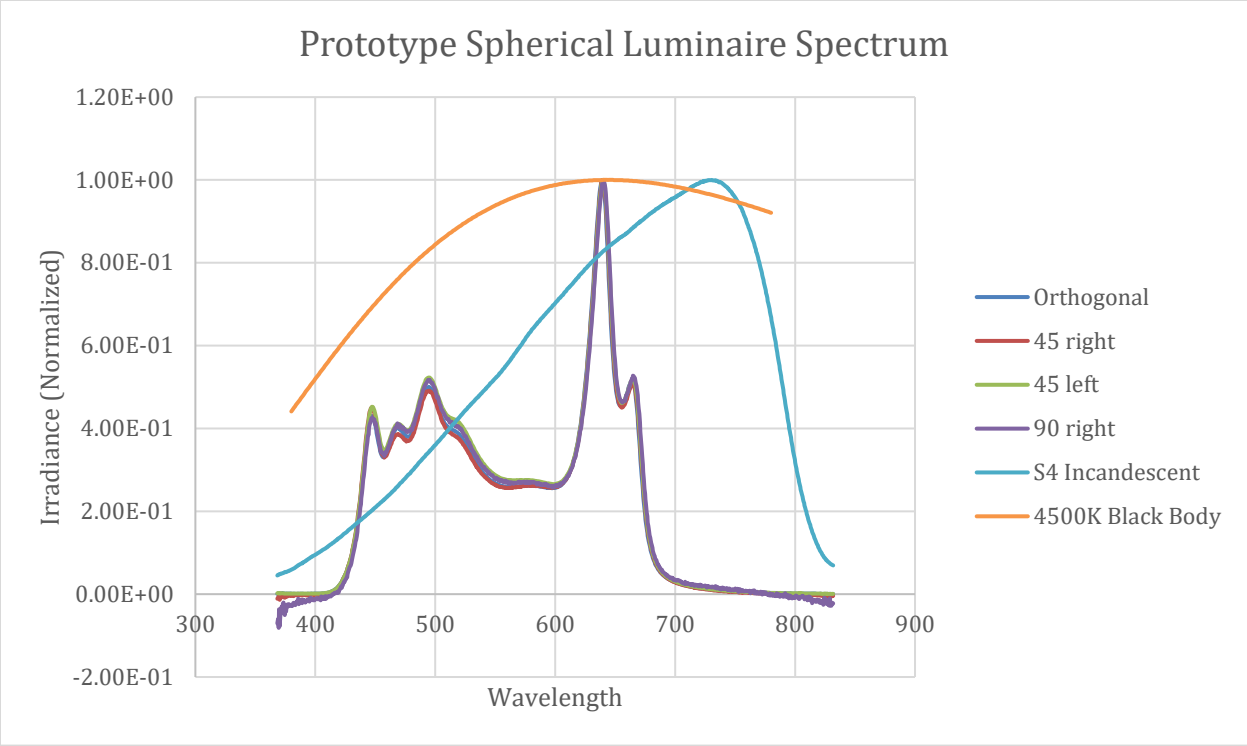

Figure 7.19: Spherical luminaire and incandescent spectrums.

Additionally, the spectrum of the spherical luminaire was recorded using the same method used for obtaining the original paint sample spectra. Readings from the spectrometer were taken orthogonally, as well as +/- 45° from the sphere, as well as one 90° measurement. The spectrums of the sphere can be seen in the plot as well. There is negligible difference across all four measurements. In order to showcase the difference between a broad-spectrum source as seen in incandescent light and the homogenized light of narrow waveband color LEDs, the incandescent source spectrum (which emits at 3200K) was plotted against the sphere spectrum. Additionally, the spectrum of a 4500K black body curve is shown to demonstrate the accuracy of the LED color ratios at matching their desired spectrum.

Figure 7.20: Spherical luminaire aimed at ETC's light lab measuring wall for photometric camera measurement.

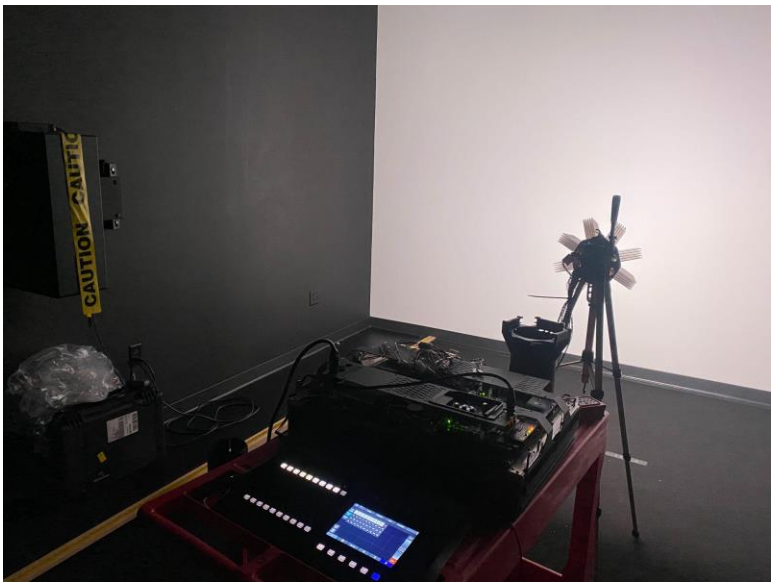

Figure 7.21: Full view of the test setup, including the Radiant Vision photometric camera mounted on the wall.

The last bit of testing done on ETC grounds was some photometric measurements done in ETC's light lab with a radiant vision photometric camera. The camera has three colors in a color wheel, and takes three consecutive pictures with each color, at an exposure level that ensures it gets adequate

photoreceptor response. The results are then summed together into one final result. Additionally, to see the feasibility of using a profile imaging lens tube, one was held in place by hand and a shot was taken.

No Lens			
	Beam Angle	97.3	
	Field Angle	NA	
	Lumens		
		Deep Red	32.3
		Red	133.8
		PC Amber	129.7
		Lime	376.5
		Green	21.9
		Cyan	127.6
		Blue	13.9
		Indigo	8
		All	843.7
With 26XDLT			236.9
			28%

Table 7.2: Results from the ETC optics lab measurements.

In ETC terms, the full-width half-maximum (50% cut off from the peak of the luminous intensity), is referred to as the beam angle, and the field angle is defined as the 10% cut off from the peak. In this case, the beam was so large that the field angle did not fit within the measurement frame.

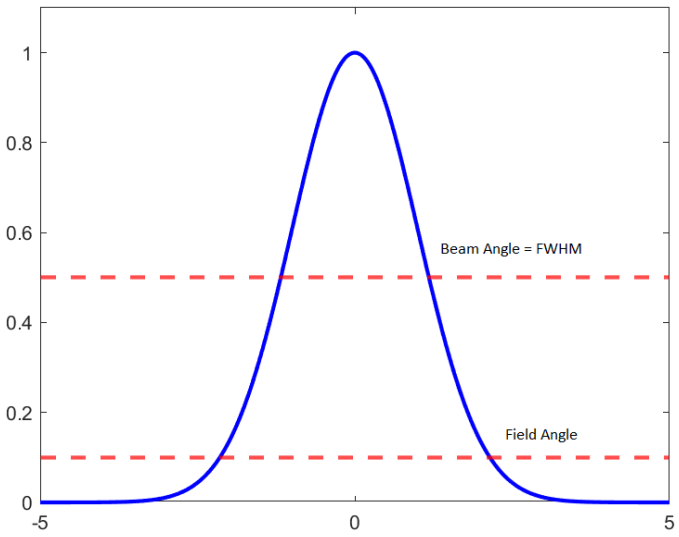

Figure 7.22: Gaussian curve demonstrating field and beam angles.

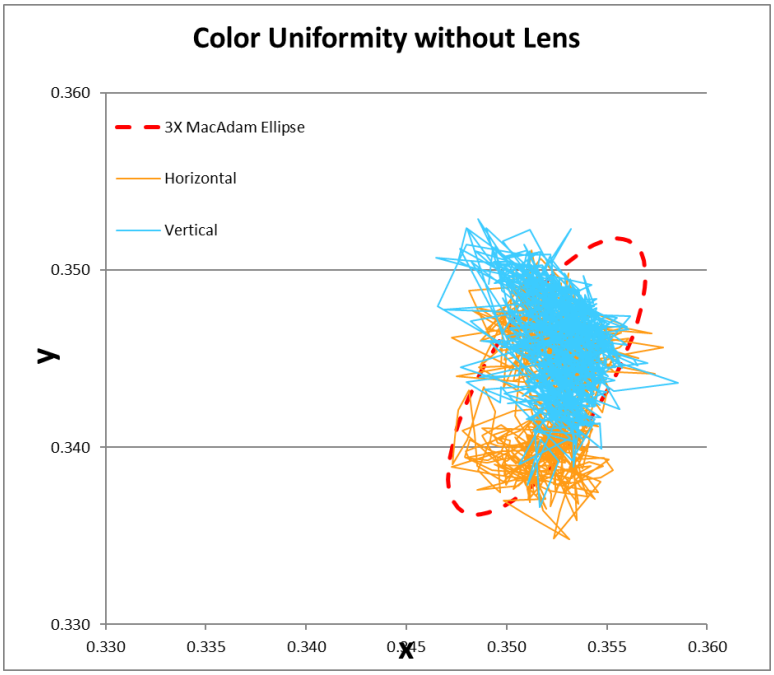

Figure 7.23: Color uniformity of the Spherical luminaire on the wall; bare fixture.

The color uniformity measured from the sphere can be considered a disappointing result. The color spread appears to be larger than a 3x MacAdam ellipse, making it worse than the Source Four LED Series 3 Lustr mix. However, there has been some internal discussion within ETC staff that the photometric camera may not be the most adequate color measuring tool due to only relying on three color filters. This has opened an investigation within the company on their equipment as they push for tighter

and tighter color uniformity requirements. ETC's ARG did provide some spectrometer measurements a few weeks after these measurements that shed a little bit of light on the issue.

Using a stepper motor/actuator in the ARG lab the CAS (CCD Array Spectrometer) optical probe traveled along a horizontal axis to sample across some fixture profiles.

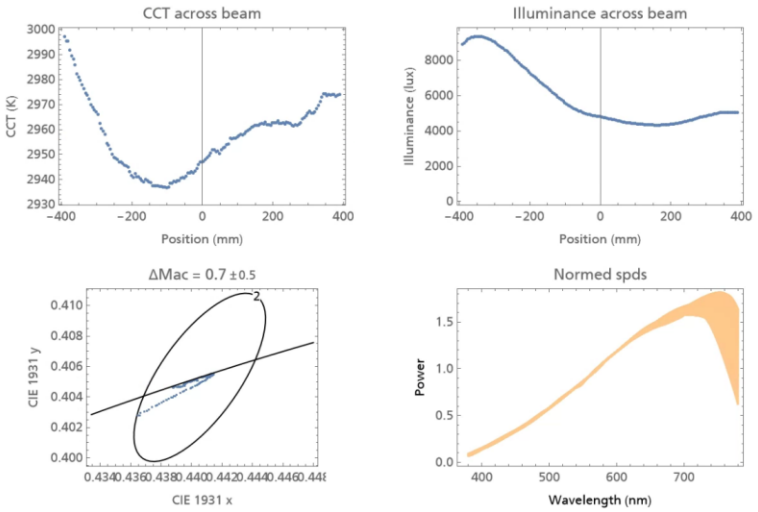

Figure 7.24: Incandescent Source ARG measurements.

This beam resulted in an approximately 70K color shift across the beam, or approximately one MacAdam.

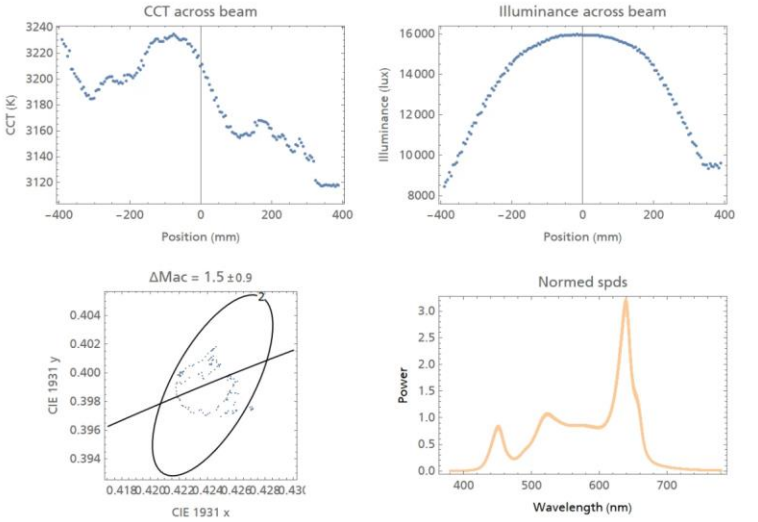

Figure 7.25: Source Four LED Series 3 ARG measurements.

The premier ETC LED fixture measured roughly 120K shift, or slightly under 2 MacAdams.

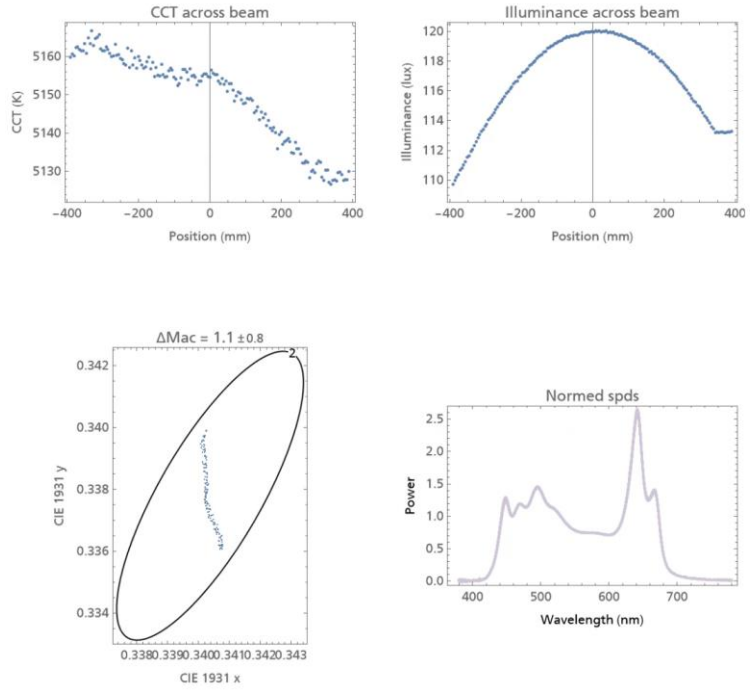

Figure 7.26: Spherical Luminaire ARG measurements.

For the spherical luminaire, color uniformity was not quite as good as the tungsten, but was better than the Series 3.

Additionally, it should be noted that with the malfunctioning Lime color LED, the color uniformity of this sphere may also just be compromised. This is something that will have to be addressed with a new board or second prototype sphere.

26 XDLT Held-by-hand measurement

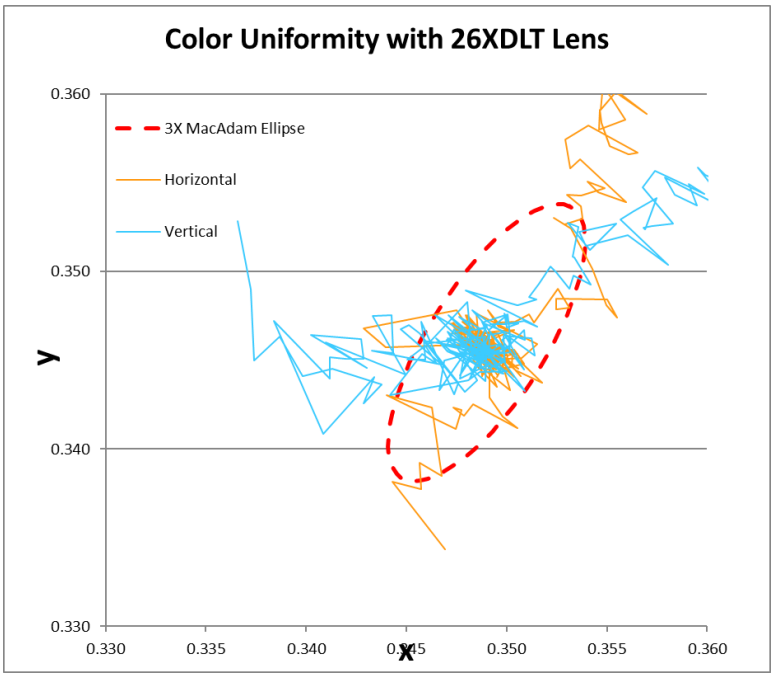

Figure 7.27: Color uniformity of the beam from the 26 XDLT lens tube held by hand in front of the spherical luminaire port.

The 26 XDLT measurement can be considered a non-usable measurement, as there was no adequate equipment to fix the tube in place. Given the weight of the tube and long exposure time (5-10 seconds per color filter), that shot was not a good representation of color uniformity, as the beam on the wall was moving and shaking considerably.

However, the lumen count from this measurement does give insight into the amount of loss that would be expected without any additional collection optics.

CHAPTER 8: Next Steps

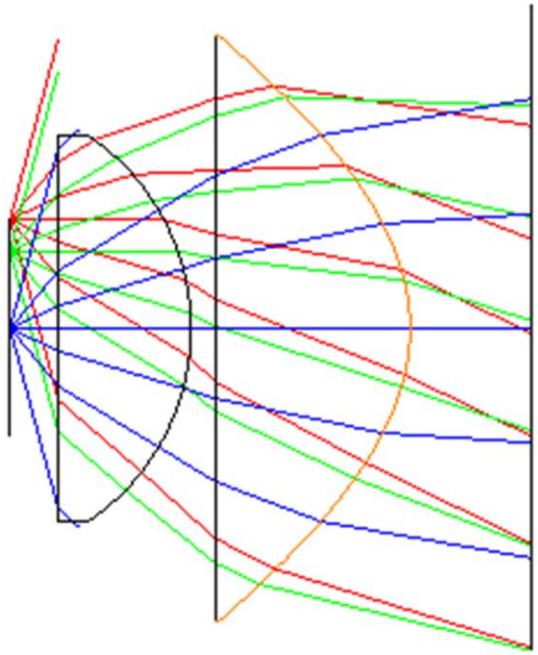

Figure 8.1: Concept of a condenser lens prescription.

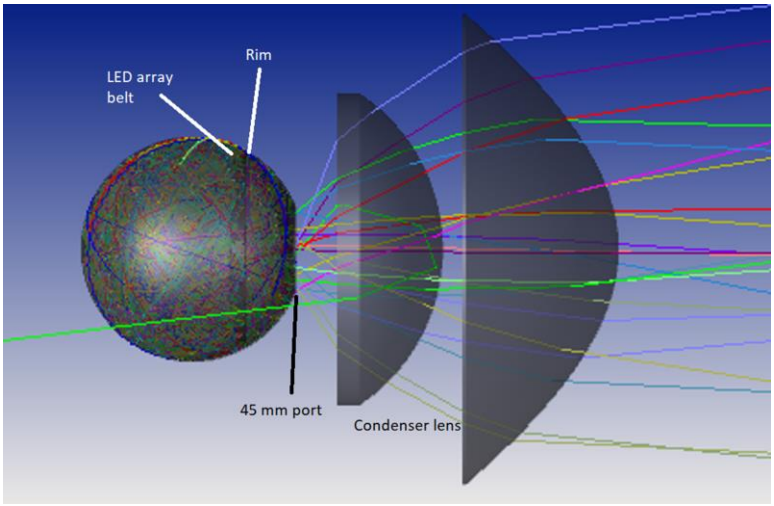

Figure 8.2: Concept for condenser lens in front of spherical luminaire.

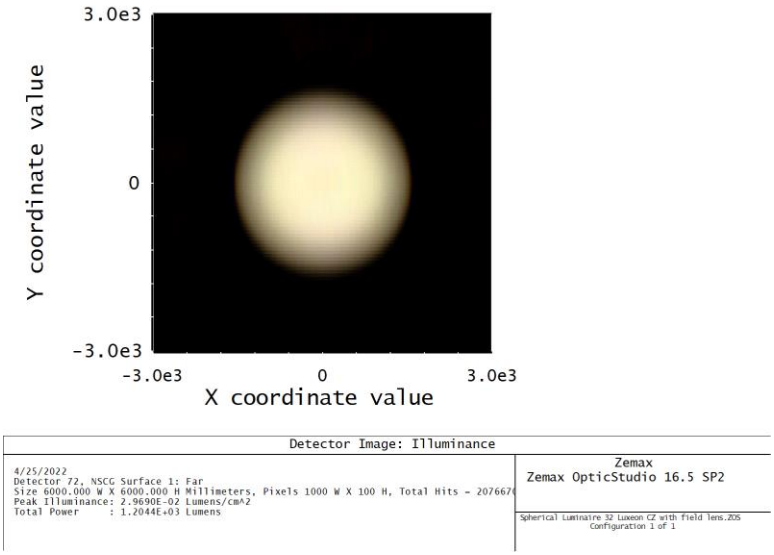

Figure 8.3: Light output projected onto a wall 3 meters away after the condenser lens.

The next step in this process is figuring out ways to collect this light. One of the initial objectives was to see if this type of light engine could serve as a good host for projection-based imaging optics, or profile lenses as referred to within the industry. However, without the aid of a reflector, CPC, etc., collecting this light for imaging would result in unacceptable losses in efficiency. Though, it can also be argued that with the spread of the LEDs, the drive current can be safely increased as cooling over the larger area would be much easier than traditional 60 to 90 piece LED arrays crammed into a small surface area.

The overall color mixing potential of this sphere was noted, and one theatrical application where it can still be very effective is in wash optics. Wash fixtures are non-imaging fixtures that aim to uniformly coat a large area with light, without a need for a hard edge in the beam. These beams are often created with the use of Fresnel lenses which are much lighter and are much more accessible to larger diameters.

CHAPTER 9: Conclusion

Contemporary theatrical LED fixtures employ many techniques to achieve the best possible color uniformity possible as well as having a spectral response across the entire visual spectrum. Many of the techniques used for color uniformity have resulted in longer and potentially unwieldy fixtures. In order to address these concerns, research was done into the viability of using a hollow cavity spherical luminaire with a white internal coating to scatter and mix the light before emitting it outward. The spherical luminaire proved a huge success in achieving color uniformity, surpassing the beam homogenization currently produced by the ETC premier line of fixtures. Initially the concept included using this spherical luminaire to feed into projection-based imaging optics, however, this concept proved to be unsatisfactorily inefficient without additional collection optics work. This concept could find its strength in wash style fixtures, which are less sensitive to light loss. These fixtures often use a Fresnel lens to "wash out" the light toward the wall, and don't require lenses to be focused. It should be noted though, that the overall output through the fixture can still be increased by adding more belts of LEDs.

There are still many questions left in this project. There are still many different types of white paints that can be tested, as seen in some of the reflectance graphs, the reflectance across the spectrum wasn't always consistent, and even the second-best reflective paints were still close to 10% less reflective than Spectralon. Finding the right coating at the right cost will be crucial in both increasing system efficiency and remaining commercially viable as a product line. On the manufacturing side, there are many logistics that will need to be answered, including better ways to assemble the sphere and see if shorting out the PCB will turn into a recurring issue.

The work provided in this research will prove to be a strong foundation for which further research into this technology can be conducted by ETC's ARG and optical engineers. If realized, this technology may bring theatrical fixtures to a new tier of color homogenization.

REFERENCES

Koshel, J. (2022). *OPTI 585 Notes: Etendue* [Review of *OPTI 585 Notes Etendue*].

Palmer, J. M., & Grant, B. G. (2009). *The art of radiometry*. SPIE Press.

Wynn, C. (2006). *An Introduction to BRDF-Based Lighting* [Review of *An Introduction to BRDF-Based Lighting*]. NVIDIA Corporation. https://www.cs.princeton.edu/courses/archive/fall06/cos526/tmp/wynn.pdf

Bogdan, A. (2011). *Comparison between Digital Image Processing and Spectrophotometric Measurements Methods. Application in Electrophoresis Interpretation* [Review of *Comparison between Digital Image Processing and Spectrophotometric Measurements Methods. Application in Electrophoresis Interpretation*]. Research Gate; Applied Medical Informatics . https://www.researchgate.net/figure/CIE-1931-xyY-Chromaticity-diagram-Conversion-from-RGB-has-been-done-using-the-following_fig4_50863695

Gnam, E. (2020). *Spherical LED Array Model* [Review of *Spherical LED Array Model*]. ETC Inc.

Angle converter : degree, radian, grade, steradian, cosinus, sinus, tangent. (n.d.). Mon-Convertisseur.fr. Retrieved November 17, 2023, from https://smart-unit-converter.com/angle-converter.php

Instrument Systems CAS 140CT CCD Array Spectroradiometer. (n.d.). Konica Minolta Sensing. Retrieved December 7, 2023, from https://sensing.konicaminolta.us/us/products/cas-140ct/

Spectralon® Diffuse Reflectance Targets Durable reflectance panels for laboratory and field applications under harsh conditions. (n.d.). Retrieved November 17, 2023, from https://www.labsphere.com/wp-content/uploads/2023/02/SpectralonTargets.pdf

Metal 3D Printing Service for Custom Parts | Online Quoting. (n.d.). Www.protolabs.com. https://www.protolabs.com/services/3d-printing/direct-metal-laser-sintering/